Providing Foot Clearance during Stair Climbing with Tendon-Driven Systems: An Experimental Approach

BY

Christos Vasileiou

For the degree of Master of Science in Mechanical Engineering
at Delft University of Technology,
to be defended publicly on Tuesday November 9, 2021 at 9:30 AM.

Student number: 5029007
Thesis committee: Dr. ir. Winfred Mugge, TU Delft
Alejandro Sancho Puchades, MyoSwiss AG
Dr. ir. Aimee Sakes, TU Delft
Dr. Michael Wiertlewski, TU Delft

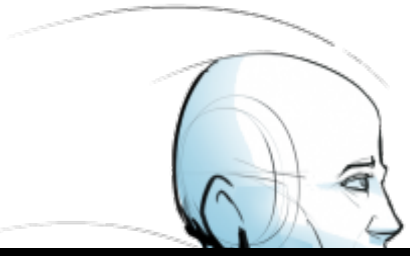

Providing Foot Clearance during Stair Climbing with Tendon-Driven Systems: An Experimental Approach

Christos Vasileiou

Thesis Report

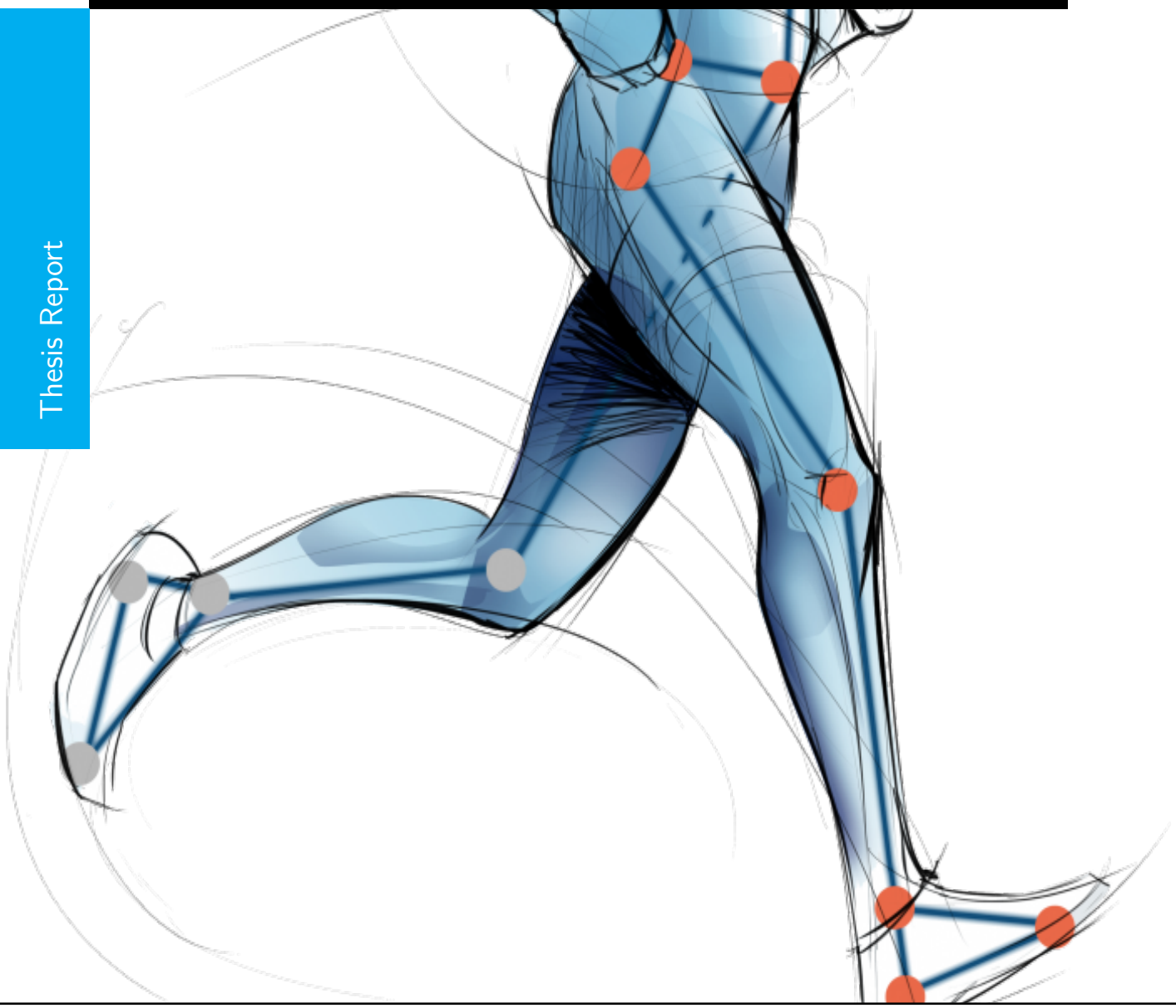

TU Delft Delft University of Technology

myoswiss

Supervisor: Alejandro Sancho Puchades

Advisor: Dr. Winfred Mugge

*Picture obtained from https://www.pngegg.com/en/png-epmox for non-commercial use

Acknowledgements

I would like to thank all the parties involved for the accomplishment of this project. Special thanks to my daily supervisor Alejandro Sancho Puchades for his guidance throughout the project and his unlimited patience. I am very grateful to the MyoSwiss team for hosting this project and for the very friendly working environment that they have created. In particular, I would like to thank Mohit, Spyros and Andri for their technical support whenever needed. Also, Gleb, Kai and Jaime for their inspiration and the insightful advice on the project. Finally, I would like to thank my TU Delft advisor, Dr. Winfred Mugge, for his valuable feedback and for challenging me to always improve my work.

Delft, University of Technology Christos Vasileiou

Providing Foot Clearance during Stair Climbing with Tendon-Driven Systems: An Experimental Approach

Christos Vasileiou[1], Alejandro Sancho Puchades[2], Dr. Winfred Mugge[1]

***Abstract*—Tendon-driven soft exosuits have gained much attention in recent years due to their ability to support people with mobility problems during daily life activities. A task that is particularly assisted by such robotic systems, due to its challenging nature, is stair climbing. However, assisting foot clearance during the swing phase of stair climbing with a tendon-driven system that actively supports hip and knee flexion has not been investigated.**

In the current study, we built a tendon-driven system to experimentally identify the foot clearance, the joint moments, the tendon forces, and the tendon velocities, that the system should provide to lift the foot above a stair-step. We experimented with able-bodied subjects that, while standing still, were instructed to keep their right leg relaxed to mimic muscle weakness. With this experimental approach, we showed how to systematically identify the basic requirements for developing an assistive device.

The system provided up to 40.1 Nm at the hip and up to 23.2 Nm at the knee when simultaneously flexing both joints, while not being constrained by any space limitations. When modified to mimic a wearable, portable exosuit, that does not protrude more than 10 cm from the body, the setup provided an average foot clearance of 17 cm with thigh tendon forces up to 455 N and shank tendon forces up to 50 N. Consequently, exosuits that support hip and knee flexion should exploit the low required shank tendon forces and the possibility of simultaneously flexing the hip and knee joints to more efficiently assist foot clearance during stair climbing.

I. Introduction

Stair climbing is a common activity of daily living (ADL), characterized as a demanding locomotor task [1]. Stair climbing, like the gait cycle, consists of a stance phase and a swing phase. The stance phase is further divided into the weight acceptance, pull-up, and forward continuance sub-phases, while the swing phase is divided into the foot clearance and foot placement sub-phases [2]. However, stair climbing can be more challenging than ground-level walking. In particular, during stair climbing, the body center-of-mass is raised, while in walking it performs a small oscillation around a specific height level. Furthermore, stair climbing requires that the foot obtains a considerable ground clearance to overcome a stair-step, while in walking the foot has to be lifted only high enough to not collide with the ground. Finally, in stair climbing, the foot placement sub-phase has to be quite precise, because wrong placement can potentially lead to falls [3]. On the other hand, during walking, the foot does not need to be precisely placed, especially when ground-level walking takes place on an even surface. As a result, considerable ranges of motion (RoM) and moments are required at the lower limb joints for accomplishing the stair climbing task [4][5].

For people with disabilities at the lower limbs, stair climbing can be cumbersome or even impossible to be accomplished. As a worst-case scenario, falling due to tripping during stair negotiation can prove fatal according to Startzell et al. [6]. The phenomenon of falling due to tripping is mainly connected to the decreased and inconsistent achievement of foot clearance, meaning that the person is not able to lift the foot high enough to overcome the next stair-step [7]. Muscle weakness, being present in several neurological disorders, such as Spinal Cord Injury (SCI), Multiple Sclerosis (MS), and Muscular Dystrophy (MD) [8], is a common cause that may be responsible for such undesired effects. The weakened muscles of people with such neurological disorders cannot consistently generate the joint moments that ensure sufficient foot clearance for stair navigation.

Currently, assistive devices can artificially ensure foot clearance to people with muscle weakness. For instance, passive orthotic devices, such as ankle-foot orthoses [9], are a simple and inexpensive solution. Alternatively, powered rigid exoskeletons have also been used during the last years [10]. The exoskeletons, being mounted on the user's lower body, prescribe the movement of the leg by applying external moments directly at the joints. Despite their great success in the field, see Rex exoskeleton [11], they are mainly constrained to research or expensive clinical facilities, due to their high complexity, size, weight, and cost [12].

A newer generation of powered assistive robots, the soft exosuits, which are defined as "clothing-like robotic devices that wrap around a person's body and work in parallel with his/her muscles" [12], are being explored. The exosuits use artificial tendons that apply forces at the leg segments to transmit flexion or extension moments to the joints. However, few studies have shown how tendon-driven exosuits interact with the wearer during stair climbing [13][14][15]. On top of that, providing foot clearance during stair climbing by actively supporting hip and knee flexion with a tendon-driven exosuit has not been investigated.

Developing a portable exosuit that supports the foot clearance phase of the stair climbing movement in people with muscle weakness is challenging for two reasons. First, the exosuit has to lift the foot higher than 22 cm, the maximum height

[1] Faculty of Mechanical, Maritime and Materials Engineering (3ME), Department of Biomechanical Engineering, Delft University of Technology, Delft, The Netherlands

[2] Myoswiss AG, Zurich, Switzerland

at which the stair-steps can reach according to standards of several countries [16]. Second, the exosuit should protrude as little as possible from the user's body, otherwise the user tends to avoid using it, as he/she feels stigmatized from a societal perspective [17]. However, when minimizing the body protrusion of a tendon-driven exosuit, the moment arms with which the artificial tendons generate moments at the joints are significantly reduced. As a result, higher tendon forces are required to provide sufficient foot clearance for stair navigation.

Hence, in the current study, we built a tendon-driven system, that can constrain the artificial tendons' body protrusion up to 10 cm, to experimentally identify four basic requirements, being the foot clearance, the joint moments, the tendon forces, and the tendon velocities, that the system should provide to lift the foot above a stair-step. The selected requirements, referred simply as requirements for the rest of the study, are the most important for determining the power demands of the system. Based on the chosen requirements, development teams can select the actuation units and the dimensions of the first portable, wearable exosuits that assist hip and knee flexion to support foot clearance during stair climbing. To identify the requirements, we experimented with able-bodied subjects that, while standing still, were instructed to keep their right leg relaxed to mimic muscles weakness. Initially, we tested five simple open-loop current controllers, without imposing space constraints on the experimental setup. Then, we tested the controller, that more efficiently provided foot clearance, by imposing space constraints on the experimental setup to mimic a wearable, portable exosuit.

Such a systematic approach that collects experimental data to identify the requirements for developing an assistive device has not been presented before. Many research groups directly develop their assistive robot without investigating beforehand its requirements in terms of forces and velocities [18][19][20][21]. For instance, Asbeck et al. [18] first designed their tendon-driven device with fixed moment arms by relying on biological joint moments, then identified the moments that were transferred at the hip joint by the artificial tendons. However, in that way, the versatility of the device is limited because they would have to build a new one in order to investigate its effect under different moment arms, in case different moments should be provided.

II. Methodology

In this section, we present the methodology that we pursued to identify the requirements of a wearable, portable exosuit that assists foot clearance by supporting hip and knee flexion. We could follow either a simulation or an experimental approach. Developed simulation methods can provide detailed information about the biomechanical behavior of the human leg [22][23]. However, when combined with a soft exosuit, the simulation environment can become quite complex. For instance, the wearable components that realize the interface between an exosuit and its wearer get displaced relatively to the leg's attachment points during actuation. As a result, additional experimental data are required to first verify the precision of the modeled interface. Such limiting factors,

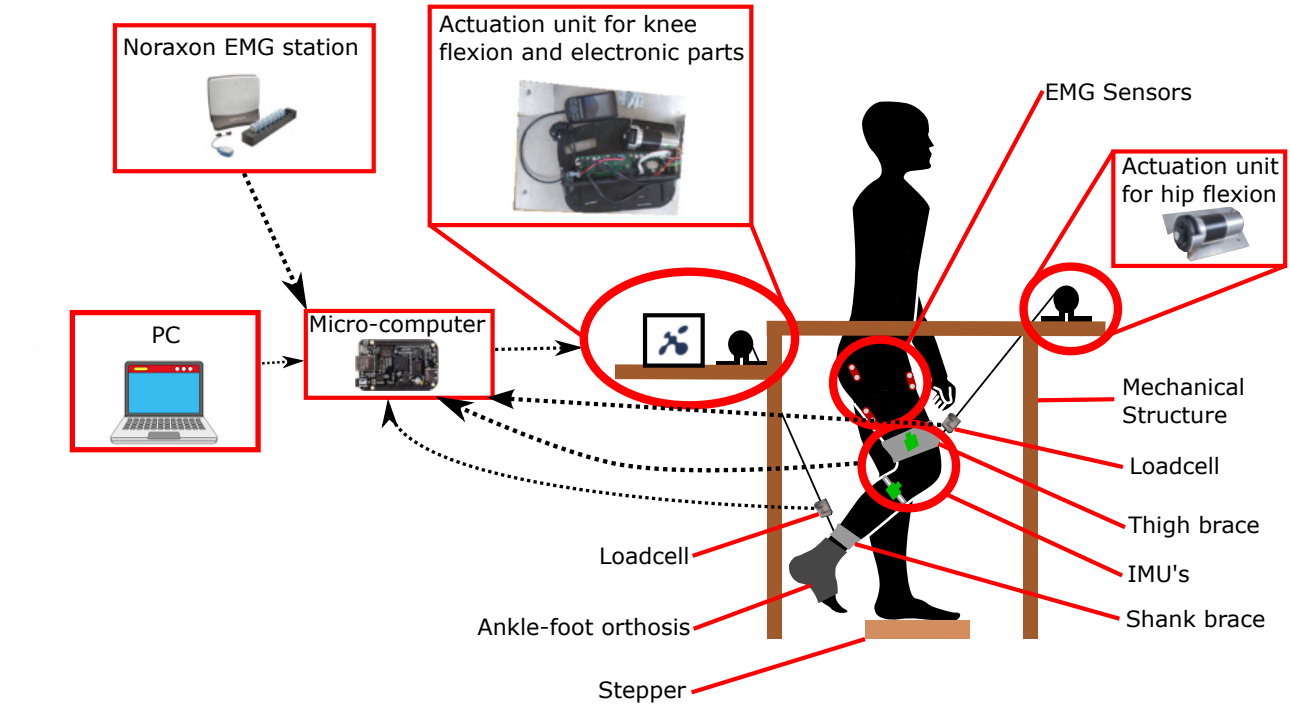

Fig. 1: Schematic representation of the experimental setup. The experimental setup is divided into the following subsystems: the mechanical structure, the wearable components, the actuation units, the sensors, and the micro-computer. The individual components of each subsystem are indicated with red lines. The black dashed arrows show the flow of the signals between the subsystems.

mainly attributed to the soft nature of the exosuits, do not allow for the development of a precise model. Therefore, we followed an experimental approach.
During the experiment, we wanted to provide foot clearance by inducing five simple movements to the leg in order to identify which movement is more efficient. Having the capability to provide foot clearance in several ways was the driving factor for the mechanical design of the experimental setup and the selection of its actuation units. Additionally, a sensor system that included loadcells, IMU sensors, and Hall sensors was integrated, in order to identify the achieved foot clearance, the generated joint moments, and the exerted tendon forces and velocities. Finally, since the experiment was conducted with able-bodied subjects, it was important that they keep their leg muscles relaxed to mimic muscle weakness. To ensure leg relaxation, we recorded the activity of selected muscles. Based on those considerations, we developed the experimental setup and designed the experimental protocol.

A. Experimental setup

The experimental setup was developed according to a simplified version of the V-model approach of the System Development Life Cycle (SDLC). Based on the V-model, we determined the needs, the design requirements, and the system specifications before developing the finalized version of the experimental setup. The process is described in more detail in Appendix A. Fig. 1 represents the setup schematically, while Fig. 2 shows the real implementation. The subsystems of the experimental setup are the mechanical structure, the wearable components, the actuation units, the sensor system, and the micro-computer.
1) Mechanical structure: The mechanical structure consisted of aluminum profiles (Strut profiles, 40x40L, Bosch Rexroth AG), that were connected with each other with angle brackets (Fig. 2). The connection was implemented with a bolt-nut pair that gave us the possibility to quickly adjust the height of the setup and the position of several components fixed on the setup (e.g. actuation units).
2) Wearable components: The wearable components included one thigh brace, one shank brace, and one ankle-foot orthosis. The thigh and the shank braces were fabricated by readjusting an off-the-shelf knee brace (CFR Folding Knee Brace - Arthritis Patella Stabilizer) made of synthetic rubber. Furthermore, we integrated a Velcro strap to fix the braces on the thigh and the shank, by adjusting their diameter. The purpose of the braces was to create an interface between the human leg and the artificial tendons. Therefore, the tendons were attached to the braces with a configuration that was created by stitching backpack universal belts (see Fig. 2). The ankle-foot orthosis was integrated with a softly padded splint made of plastic. Four fastening Velcro straps were used to hold the foot in place. The use of the ankle-foot orthosis was necessary to keep the ankle at a constant angle, in the sense that there would be no active contribution to the achieved foot clearance due to ankle dorsi-/plantarflexion during the experiment.
3) Actuation units: Two actuation units were used to provide active support at the hip and knee joints. Each actuation unit

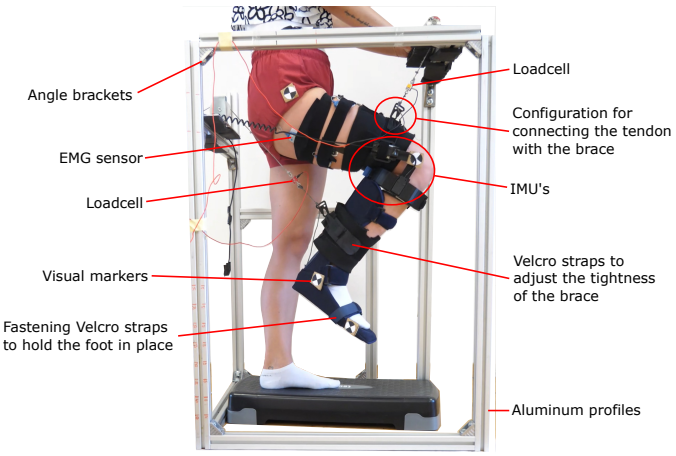

Fig. 2: Implementation of the experimental setup that actively supports hip and knee flexion. Additional details that are not visible on the schematic setup are indicated. The aluminum profiles provided structure to the setup. The interface of the setup with the human leg was realized with the use of wearable braces. The artificial tendons were responsible for applying tensile forces at the thigh and the shank that were converted into hip and knee moments. Visual markers were used to track the movement of the leg with a simple camera at the sagittal plane.

was placed on a metallic plate that was directly attached to the mechanical structure. The units incorporated a 70W brushless DC motor (Maxon EC-i40), a gearbox (gear ratio 15.16:1), and a pulley (effective diameter D=38mm). The artificial tendons, made of inelastic, abrasion-resistant Dyneema cables (Dyneema Throwline / Marlow, 0.6mm, min. break load 410kg), were fixed to the pulley of the corresponding actuation unit.
Based on the expected forces (F) that we intended to exert with the artificial tendons, we defined the motor currents (I) that should be provided by the actuation unit, according to the equation:

$$I = \frac{F \cdot r_{pulley}}{\eta \cdot \mu \cdot k_M \cdot i_{gb}} \tag{1}$$

where $r_{pulley} = 19mm$ is the effective radius of the pulley, $\eta = 0.89$ is the motor efficiency, $\mu = 0.81$ is the gearbox efficiency, $k_M = 46.1mNm/A$ is the motor torque constant, and $i_{gb} = 15.16$ is the gearbox ratio. Essentially, the provided motor current is converted into the tendon force due to the implemented gearbox and pulley system that is described in Fig. 3.
4) Sensor system: The purpose of the sensor system was to collect data for post-processing rather than creating a closed-loop control scheme. The sensor system consisted of one simple camera, two inertial measurement units (IMU's), two loadcells, two motor Hall sensors, and three EMG sensors. The camera, placed in a way to record the sagittal plane, was used to track the movement of the leg. Visual markers, placed on the participant's leg (see Fig. 2), provided additional reference points in the video recording. The two IMU's were mounted

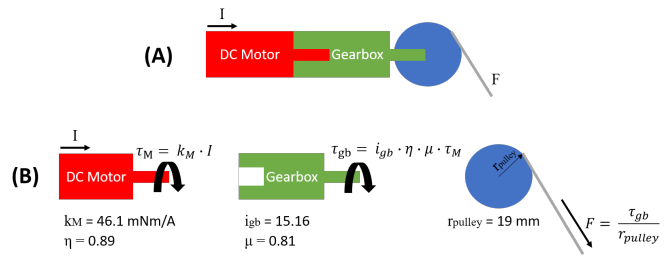

Fig. 3: (A) Schematic representation of the actuation unit. The motor current is converted into tendon force through a gearbox and a pulley. (B) Exploded view of the actuation unit. The motor current (I) is multiplied with the torque constant (k_M) to obtain the motor torque (τ_M). The motor torque is converted into gearbox torque (τ_{gb}) through the motor efficiency (η), the gearbox ratio (i_{gb}) and efficiency (μ). Finally, we obtain the tendon force (F) with the use of the pulley (colored in blue).

on the thigh and the shank. Each IMU was enclosed in a small box to be protected from the outer environment. The selected loadcells (FUTEK, LSB200/QSH01905, Miniature S-beam Jr., maximum capacity 445 N, minimum resolution 0.4 N) could directly measure the tensile forces exerted by the tendons. The Hall sensors were integrated in the DC motors to record the counts of the motor. Finally, the EMG sensors (Ultium EMG Sensor System, Noraxon, Scottsdale, AZ, USA) were used to measure the muscle activity of the Rectus Femoris (RF), the Biceps Femoris (BF), and the Gluteus Maximus (GM). The three muscles were selected because they are either hip flexors/extensors or knee flexors/extensors. Consequently, they either support or resist obtaining foot clearance during stair climbing. The EMG sensors, being wireless, could transmit signals to the main station at 2000 Hz. Hydrogel/Ag/AgCl surface electrodes (Kendall Arbo H124SG, Covidien, Ireland) were placed in a bipolar configuration over the three selected muscles following standard procedures [24].

5) Micro-computer: The experimental setup was controlled by one ARM A8 micro-computer unit (BeagleBone; AM335x 1GHz ARM Cortex-A8; programming language C). The unit was responsible for sending commands to the motors at 100 Hz, receiving data from the sensors, and synchronizing with the EMG station via an audio cable. A USB cable was used to connect the unit with a personal computer for programming (Cloud9 IDE environment). Finally, the power source of the unit was ensured with an external battery.

B. Participants

Four unimpaired males and four unimpaired females were recruited as a local convenience sample. The subjects participated in the study after they gave their informed consent. The recruitment process of the participants was done according to the inclusion and exclusion criteria of Table I. Participant characteristics are presented in Table II. For anonymization purposes, an ID from P1 to P8 was attributed randomly to each participant. The detailed characteristics of each participant are given in Appendix C.

TABLE I: Inclusion and exclusion criteria

Inclusion criteria	Exclusion criteria
Age between 19 and 64 years old	Mobility problems
Body height between 150 and 195 cm	Neurological disorders
Body weight between 50 and 95 kg	Genetic disorders

TABLE II: Age, weight, and height of unimpaired study participants.

Unimpaired Participants	Mean (SD)	Min.	Max.
Age (yrs)	27 (2.6)	24	30
Weight (kg)	64.7 (11.4)	50.9	85.7
Height (cm)	173 (11.2)	161	195

C. Experimental protocol

The experimental setup and protocol were approved by the Human Research Ethics Committee of the Delft University of Technology. The primary goal of the experiment was to identify the basic requirements, being the foot clearance, the joint moments, the tendon forces, and the tendon velocities, that should be provided by the system to lift the foot above a stair-step. However, the requirements depend on the specific joint that is actuated and the sequence with which the actuation is provided. For instance, the hip moment would not be the same in the case where only the hip joint is actuated from the case where both the hip and knee joints are actuated simultaneously or the case where the hip joint is actuated with the knee joint being already flexed. Similarly, the knee moment would not be the same in the case where only the knee joint is actuated from the case where both the hip and knee joints are actuated simultaneously or the case where the knee joint is actuated with the hip joint being already flexed.

With the performed experiment we intended to identify the system's requirements for five simple movements of the leg. We started experimenting with simple movements in order to find which is more efficient, meaning which required lower moments at the hip and knee joints. Based on our findings, the selected movement could be further analyzed and optimized in future studies, according to more specific criteria, such as movement naturalness or highest reduction of metabolic cost. Subsequently, we implemented, in the same order for all participants, five simple open-loop current controller alternatives:

- **'Simultaneous' alternative**. In this alternative, currents from both actuation units for hip and knee flexion were applied simultaneously,
- **'Hip - knee' alternative**. In this alternative, first the hip actuation unit applied currents up to the maximum level. Then the knee actuation unit applied currents while keep-

ing the currents from the hip actuation unit at maximum level,

- **'Knee - hip' alternative**. In this alternative, first the knee actuation unit applied currents up to the maximum level. Then the hip actuation unit applied currents while keeping the currents from the knee actuation unit at maximum level,
- **'Only hip' alternative**. In this alternative, currents only from the hip actuation unit were applied, and
- **'Only knee' alternative**. In this alternative, currents only from the knee actuation unit were applied.

The implemented controller alternatives can provide useful results for research groups that are interested in developing only hip flexor exosuits or only knee flexor exosuits, or hip and knee flexor exosuits.

The experiment was conducted under two configurations of the experimental setup. In the first configuration, called 'Big moment arm configuration' for the rest of the study (see Fig. 4(A)), all five controllers were tested. The goal was to identify the moments that the tendon-driven system should provide to lift the foot above a stair-step. The moments were generated by the system through the application of tendon forces at the thigh and shank segments. However, to lift the leg at a considerable height, high forces, that were not known beforehand, should be provided. To ensure that the tendon forces generated by the actuation units would be sufficient for lifting the leg, the forces should be applied normally to the leg segments at the position of the leg that requires the highest moments. In that way, the moment arms are maximized resulting in higher generated joint moments with the same tendon forces. Based on this consideration, the positions of the motors, given in Table III, were determined. The detailed calculations are provided in Appendix B.

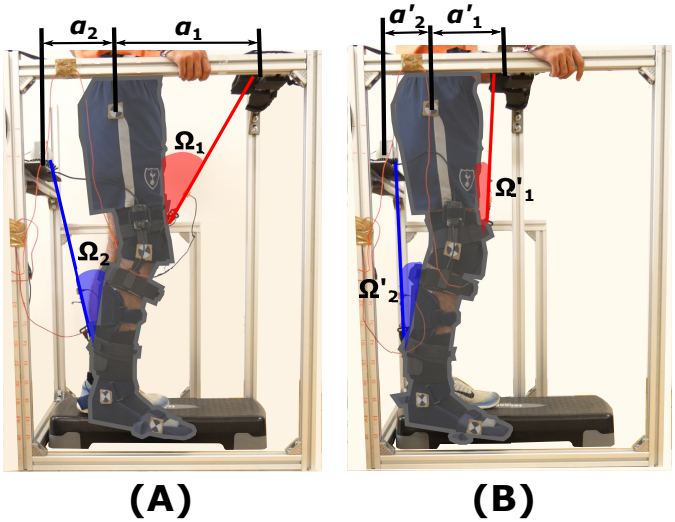

Fig. 4: (A) 'Big moment arm configuration' of the experimental setup. The positions of the actuation units were selected so as to apply the tendon forces normally to the leg segments at the position of the leg that requires the highest joint moments. Selecting carefully the correct positions of the actuation units was critical because the exact magnitude of tendon forces that should be provided was not known beforehand, so the moment arms should be maximized to ensure that the leg could be lifted. (B) 'Small moment arm configuration' of the experimental setup. We intended to identify the tendon forces and velocities that should be provided by the actuation units when approximating the behavior of a wearable, portable exosuit. Knowing the tendon forces and velocities was critical for sizing the actuation units, based on which the first potential implementations of wearable, portable exosuits can be proposed. When switching from the 'big moment arm configuration' to the 'small moment arm configuration', the distances a_1 and a_2 were decreased to $a_1^{'}$ and $a_2^{'}$ respectively. Similarly, the angles (Ω_1 and Ω_2) between the tendons and the leg (indicated with red and blue color) were decreased, resulting in smaller moment arms.

In the second configuration, called 'Small moment arm configuration' for the rest of the study (see Fig. 4(B)), we tested the most efficient controller under space constraints of the experimental setup. The most efficient controller was selected as the controller that generated lower moments at both joints to provide at least 22 cm of foot clearance with the 'big moment arm configuration'. In the 'small moment arm configuration', the maximum moment arms with which the artificial tendons generated joint moments during the leg's movement were set to 16 cm for the thigh tendon and 26 cm for the shank tendon. The specific moment arms were achieved by selecting the horizontal distances between the hip joint and the actuation units as shown in Table III. The moment arms and the positions of the actuation units were selected to approximate the behavior of a wearable, portable exosuit. A wearable, portable device should protrude from the body as little as possible [17], otherwise the users tend to avoid using it, because they feel stigmatized. To reduce the body protrusion, the motors should be placed very close to the body.

TABLE III: Positions of the actuation units with respect to the hip joint.

Moment arm configuration	**Big**	**Small**
Horizontal distance between hip actuation unit and hip joint (anterior to the hip)	38 cm	15 cm
Vertical distance between hip actuation unit and hip joint (above hip joint)	5 cm	5 cm
Horizontal distance between knee actuation unit and hip joint (posterior to the hip joint)	17 cm	11 cm
Vertical distance between knee actuation unit and hip joint (below hip joint)	9 cm	9 cm

As a result, the moment arms with which the artificial tendons generate moments around the joints are reduced. Therefore, the actuation units have to provide higher forces to compensate for the reduced moment arms. Thus, with the 'small moment arm configuration', we aimed at identifying the maximum tendon forces and velocities, as they are the necessary information to determine the size of the actuation units of an exosuit.

In each controller alternative, the left foot of the participant was placed on a stepper, while the right foot was floating from an initial position (see Fig. 4). The forces (F) applied by the artificial tendons were controlled by defining the current (I) at the DC motor of the actuation units, according to equation 1. Each alternative was repeated 15 times in total (five repetitions with low motor currents, five repetitions with medium motor currents, five repetitions with high motor currents). From the five repetitions of each motor current level, two were used for participant's familiarization with the system, while the latter three repetitions were used for data processing. Each repetition included two phases: 1) the loading phase lasting 5s, in which the leg was raised, 2) the unloading phase lasting 2s, in which the leg returned to the initial position. However, the required currents to provide sufficient foot clearance were not known beforehand. We calculated a first estimation of the maximum currents by using our simple static model (I_{model}), given in Appendix B. Based on the maximum current, we implemented a ramp to gradually increase the applied motor current from 0 to the maximum value for the first five repetitions. The linear ramp was selected, to ensure smooth application of forces that would decrease the tendency of the participants to contract their muscles non-voluntarily. Avoiding non-voluntary contractions was critical for mimicking subjects with muscle weakness. However, since a static model was used, the predicted maximum currents would not be sufficient for providing foot clearance of at least 22 cm. Therefore, by implementing software and hardware thresholds for safety reasons, we scaled up the motor currents; with a factor of 2 for repetitions 6 to 10, with a factor of 3 for repetitions 11 to 15, as shown in Fig. 5.

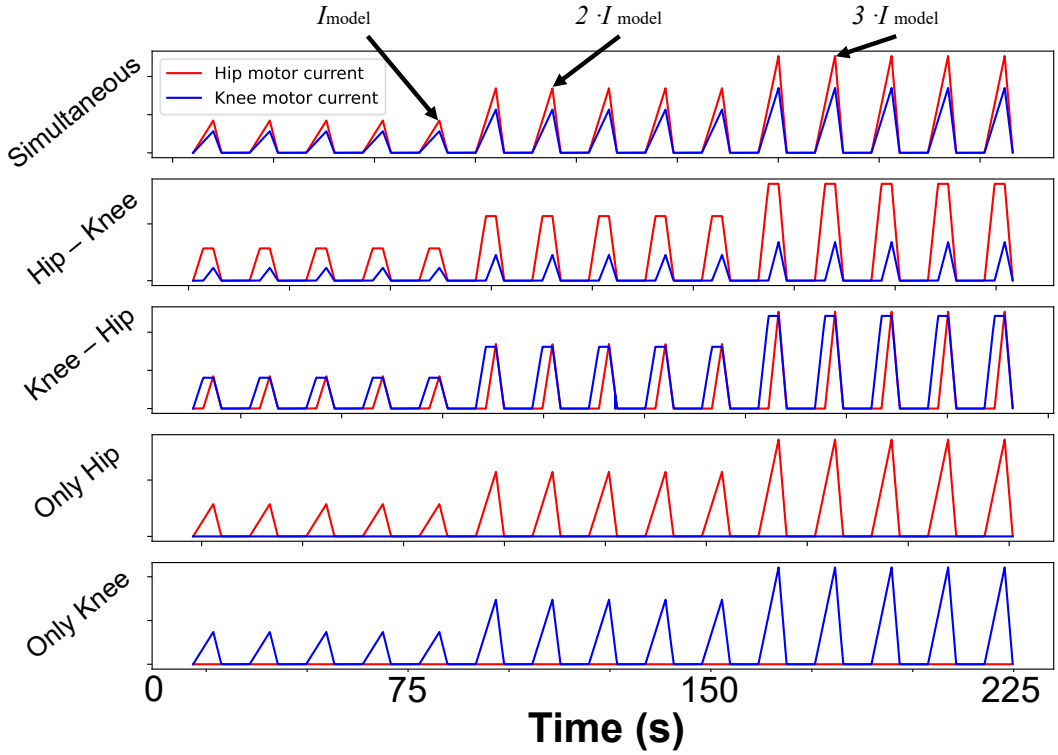

Fig. 5: Motor currents provided as input from the actuation units for the 5 controller alternatives. Each alternative was repeated 5 times with low motor currents, predicted by the static model (I_{model}), 5 times with medium motor currents ($2 \cdot I_{model}$), 5 times with high motor currents ($3 \cdot I_{model}$). The maximum currents were not the same for each participant because the model was individualized by taking into account the participants' characteristics given in Appendix C. In addition, the scaling of the currents was not the same among the controller alternatives because the tendon forces that should be provided would change for each alternative. For instance, in the 'hip-knee' alternative, first the hip joint is actuated, therefore higher forces are required as the weight of the shank creates a big moment arm around the hip joint. On the contrary, in the 'knee-hip' alternative, the hip motor current is comparable to the knee motor current. That happens, because hip flexion takes place when the knee is already flexed. As a result, the weight of the shank creates a small moment arm around the hip joint, therefore smaller forces are required from the thigh tendon. The currents were applied with a sawtooth pattern to ensure smooth application of forces that would decrease the tendency of the participants to contract their muscles non-voluntarily.

The activity of the participants' leg muscles was tracked with EMG sensors to verify whether they had their leg relaxed. The recorded muscle activity was later normalized to the reference values of a baseline measurement. During the baseline measurement, a voluntary contraction task was performed, in which the participants were asked to lift three times their foot for more than 22 cm (the maximum height at which the stair-steps can reach according to standards of several countries [16]) by flexing the hip and knee joints without any assistance from the system while wearing the ankle-foot orthosis.

D. Data processing

Synchronously recorded IMU, loadcell, Hall sensor, and EMG data were post-processed offline in Python (Python Software Foundation. Python Language Reference, version 3.8) for further analysis. From each motor current level, the loading phase (increase of the motor current from 0 to maximum value) of the last three repetitions was taken into account for post-processing. The average and the standard deviation of the data were calculated from the three non discarded repetitions of each motor current level.

Measurements from the IMU's were used to determine the thigh (θ_1) and shank angles (θ_2). To extract the angles from the IMU's, an algorithm developed by MyoSwiss AG was applied. The thigh and shank angles were used to calculate the displacement of the foot (x_f, y_f), according to the anthropometric data of each participant (see Appendix C) and the following kinematic equations:

$$x_f = l_1 \cdot \cos\theta_1 + l_2 \cdot \cos\theta_2 + l_3 \cdot \sin\theta_2 \tag{2}$$

$$y_f = l_1 \cdot \sin\theta_1 - l_2 \cdot \sin\theta_2 + l_3 \cdot \cos\theta_2 \tag{3}$$

The foot clearance (FC) was determined by calculating the height difference of the foot tip at the final position of the leg and the zero ground level, which was considered to be the stepper. The tendon forces were directly measured by the loadcells attached to the tendons. The moment at the hip joint (M_1) was calculated as a flexion moment due to the thigh tendon force (F_1) and an extension moment due to the shank tendon force (F_2). The moment at the knee joint (M_2) was calculated as a flexion moment due to the shank tendon force (F_2). The calculations are depicted in the following equations:

$$M_1 = F_1 \cdot \sin\psi_1 \cdot d_1 - F_2 \cdot \sin\xi \cdot \sqrt{a_2^2 + b_2^2} \tag{4}$$

$$M_2 = F_2 \cdot \sin\psi_2 \cdot d_2 \tag{5}$$

The angles and lengths that have been used in equations 2-5 are represented in Fig. 6. More detailed calculations that show how each variable is further determined are given in Appendix B. The motor counts (c), given by the Hall sensors, along with the specifications of the actuation unit (r_{pulley} and i_{gb}), were used to calculate the average tendon velocity (v), according to the equation:

$$v = \frac{c \cdot r_{pulley}}{2\pi \cdot i_{gb} \cdot \Delta t} \tag{6}$$

where Δt is the total movement time.

EMG raw data were filtered with a second-order bandpass filter (passband between 20Hz and 400Hz), rectified, smoothed by determining the root-mean-square value over a moving window of 200ms, and normalized to reference values [21]. The reference values were calculated as the maximum of the root-mean-squares of the signals obtained during the voluntary contraction task [25]. The EMG signals were used to show whether the participant was able to relax enough his leg to mimic muscle weakness. However, there is not a specific threshold that indicates muscle weakness, according to the muscle force of a person. The residual muscle force depends on the neurological disorder and the specific motion of the lower limb joints [26]. For instance, post-stroke patients, during hip and knee flexion tasks, were able to provide with their affected leg 25% - 65% of the joint moments that their non-affected leg provided [26][27]. Similarly, Chung et al. [28] showed that the joint moments of people with multiple sclerosis were approximately 25% of the moments of able-bodied subjects. Subsequently, accounting for the lowest thresholds, we assumed that subjects that participated in our experiment without activating their muscles more than 25% were able to mimic muscle weakness. Hence, for our results we used only data from participants that activated the recorded muscles less than 25%, while the rest of the participants were excluded from the analysis.

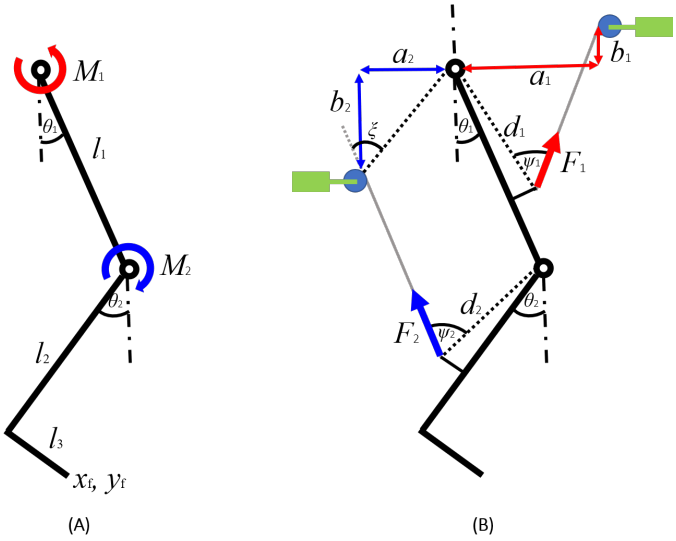

Fig. 6: (A) Schematic representation of a human leg in the sagittal plane. The lengths l_1, l_2, and l_3 are anthropometric data measured on the participants (see Appendix C). (B) Geometric configuration of the tendon-driven setup on the schematic leg along with the system's actuation units (the green boxes represent the motor and the gearbox, while the blue circles represent the pulley). The moments that are generated at the hip (M_1) and knee (M_2) joints, shown in (A), are calculated from the tendon-based geometry and the tendon forces F_1 and F_2, shown in (B), according to the equations 4 and 5.

III. Results

A. Big moment arm configuration

1) Foot clearance: From the three motor current levels, applied during the experiment, only the third level could lift the foot of all participants more than 22 cm, the maximum height at which the stair-steps can reach according to standards of several countries [16]. Therefore, only data from the high current level were used for further analysis.

Each of the five tested controller alternatives generated different leg motions at the high motor current level, as represented with the snapshots of Fig. 7, where the movement of the leg is shown for a single participant. The horizontal and vertical displacement of the foot, calculated from the IMU angles of the thigh and the shank, see Fig. 8(A), were combined in a plot, Fig. 8(B), to demonstrate the displacement of the foot tip for the five implemented controller alternatives. The maximum vertical displacement of the foot that was achieved corresponds to the foot clearance at the final configuration of the leg. Among the five controller alternatives, the minimum foot clearance, being 23 cm, was achieved with the 'only hip' alternative, while the maximum foot clearance, being 34 cm, was achieved with the 'only knee' alternative.

2) Moments generated at the joints: To determine the efficiency of the controller alternatives, we identified the moments generated at the joints by the tendons. The moments were calculated from the forces recorded by the loadcells, the maximum values of which are represented with boxplots in Fig. 9. Accordingly, the maximum values of the moments among the participants are shown with boxplots in Fig. 10.

Overall, the generated moments at the hip and knee joints would change according to the controller alternative. The ranges of moments provided at the hip joint were similar for the 'simultaneous' (9.4 - 40.1 Nm) and 'knee - hip' alternatives (13.2 - 32.8 Nm), while higher hip moments were obtained for

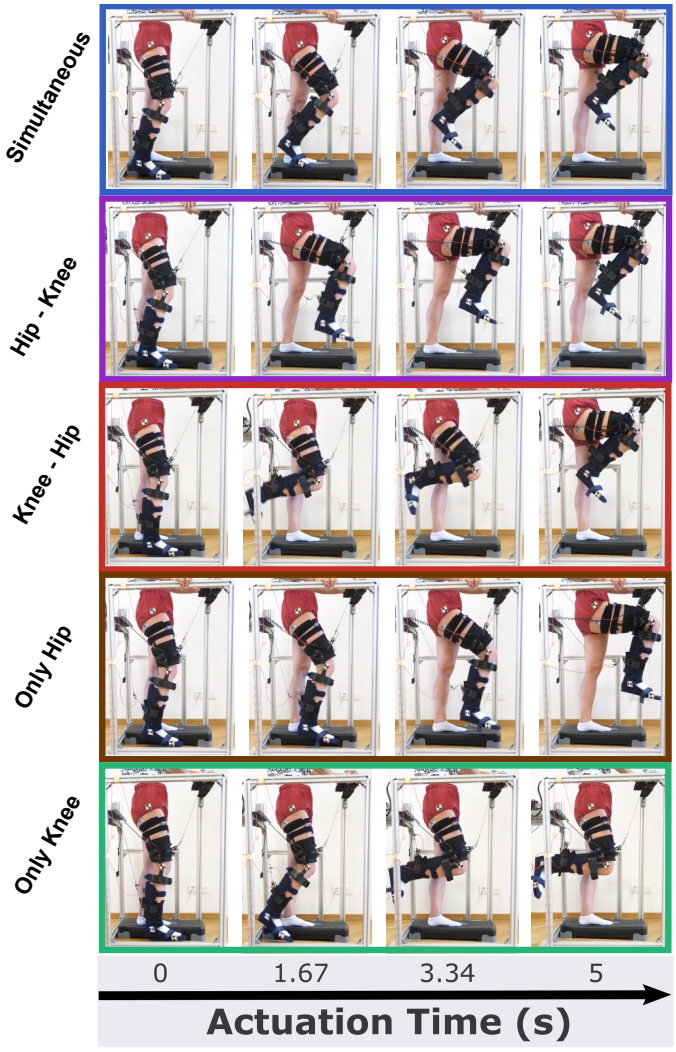

Fig. 7: Movement of the leg demonstrated through a sequence of snapshots. The five rows of snapshots correspond to the five implemented controller alternatives, as indicated by the labels at the left of the figure.

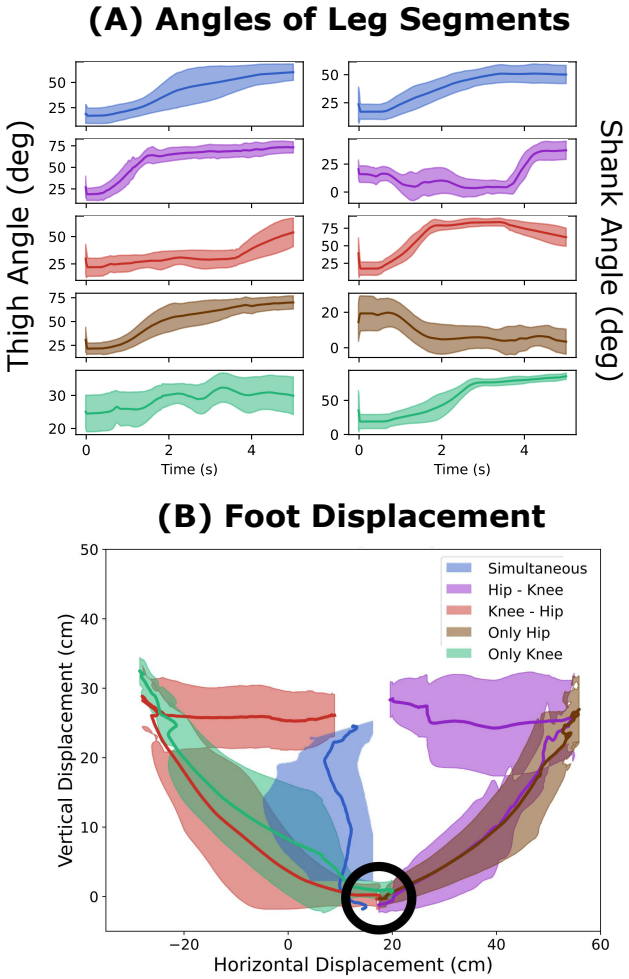

Fig. 8: (A) Thigh and shank angles of participants during the experiment. The average and the standard deviation of the participants' angles are represented with a thick line and a shaded area respectively. (B) The displacement of the foot is represented in the 2D space. The black circle shows the initial position of the foot. The same color code is followed for the five alternatives of foot clearance.

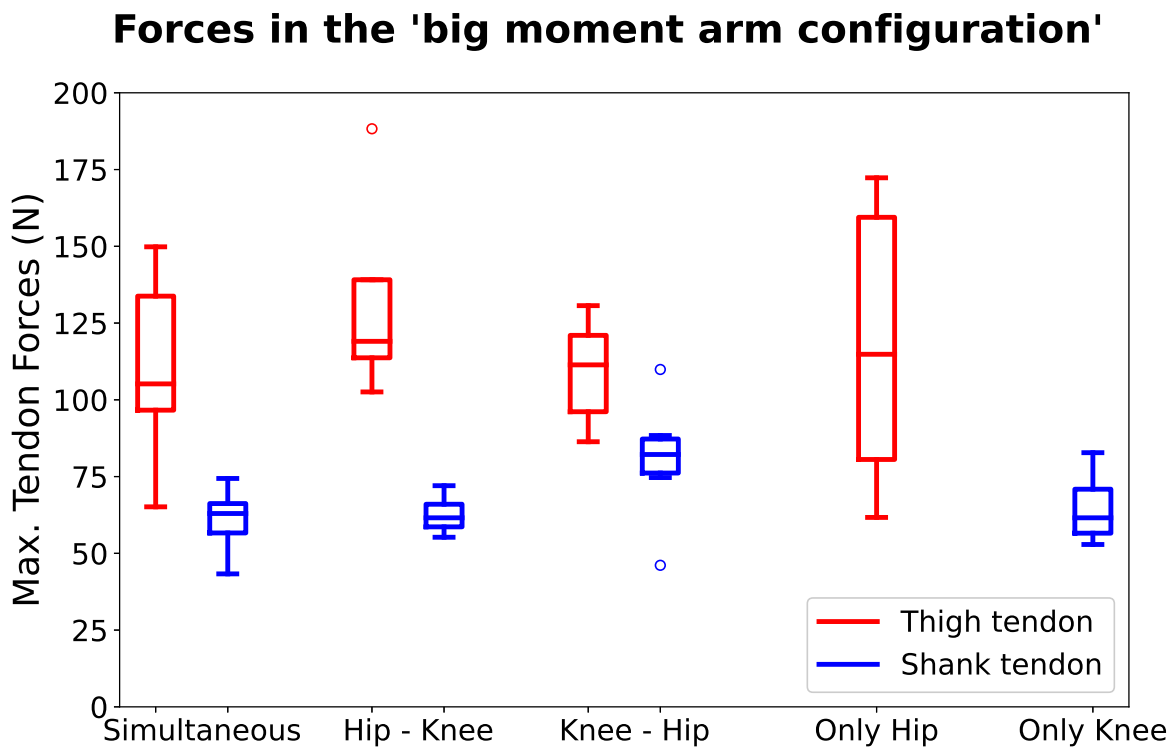

Fig. 9: The boxplots represent the maximum forces exerted by the tendons during foot clearance among the participants. Data shown for the five implemented controllers in the 'big moment arm configuration'. Red boxplots correspond to thigh tendon forces, while blue boxplots correspond to shank tendon forces.

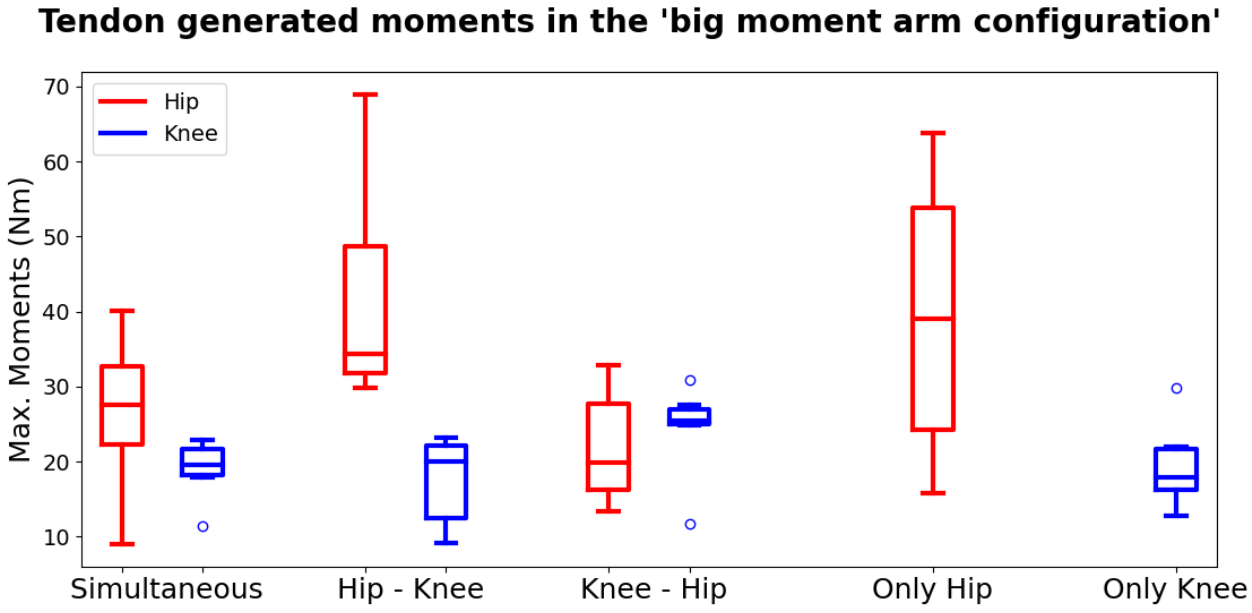

Fig. 10: The boxplots represent the maximum joint moments that were generated by the tendons during foot clearance. The red boxplots represent the moments at the hip, while the blue boxplots represent the moments at the knee. The maximum provided hip moment among the participants was noticed at the 'hip - knee' alternative (69 Nm), while the maximum knee moment was noticed at the 'knee - hip' alternative (31 Nm). The tendon-driven system was able to generate the required moments with two 70 W actuation units.

the ‘hip - knee’ (up to 69 Nm) and ‘only hip’ (up to 63.9 Nm) alternatives. Regarding the knee joint, the highest moments were obtained for the ‘knee - hip’ (11.6 - 31 Nm) and ‘only knee’ (12.8 - 29.8 Nm) alternatives, while the lowest was for the ‘simultaneous’ (11.4 - 23.2 Nm) and ‘hip - knee’ (9.3 - 23.4 Nm) alternatives.

Similarly to the joint moments, higher thigh tendon forces were obtained for the ‘hip - knee’ (up to 188 N) and ‘only hip’ (up to 172.3 N) alternatives, while the ‘simultaneous’ (up to 149.8 N) and ‘knee - hip’ (up to 130.7 N) alternatives required lower thigh tendon forces. Regarding the shank tendon forces, the ‘knee - hip’ alternative achieved the highest forces (up to 110 N), while lower forces were achieved with the ‘simultaneous’ (up to 74.4 N), ‘hip - knee’ (up to 72 N), and ‘only knee’ (up to 82.8 N) alternatives.

3) EMG activity: To ensure that the processed data refer to participants with low activity at their lower limbs, we analyzed the recorded EMG signals of the unimpaired participants. In total, we had 120 muscle recordings, given that 8 subjects participated in all five alternatives of leg elevation, while three muscles were recorded from each subject. The muscle recordings are represented in Fig. 11, in which the maximum normalized EMG activity with respect to the baseline measurement is represented with boxplots.

We excluded participants that had normalized EMG activity (averaged over the three leg elevation repetitions) higher than 25% in any of the recorded muscles, as explained in Section II-D. The exclusion was performed individually for each controller alternative, see Table IV. Overall, we excluded two participants from the ‘simultaneous’ alternative, three participants from the ‘hip - knee’ alternative, two participants from the ‘knee - hip’ alternative, two participants from the ‘only hip’ alternative, and one participant from the ‘only knee’ alternative. Only the data of the non-excluded participants were used for post-processing.

B. Small moment arm configuration

1) Foot clearance: We were able to achieve (17 ± 8) cm of foot clearance with the experimental setup in the ‘small moment arm configuration’. The main limitations of the achieved foot clearance were space constraints rather than power constraints. As shown in Fig. 12, the thigh loadcell (in the purple circle) reached the actuation unit. As a result, the motor was not able to further rotate in order to increase the angle of the hip joint.

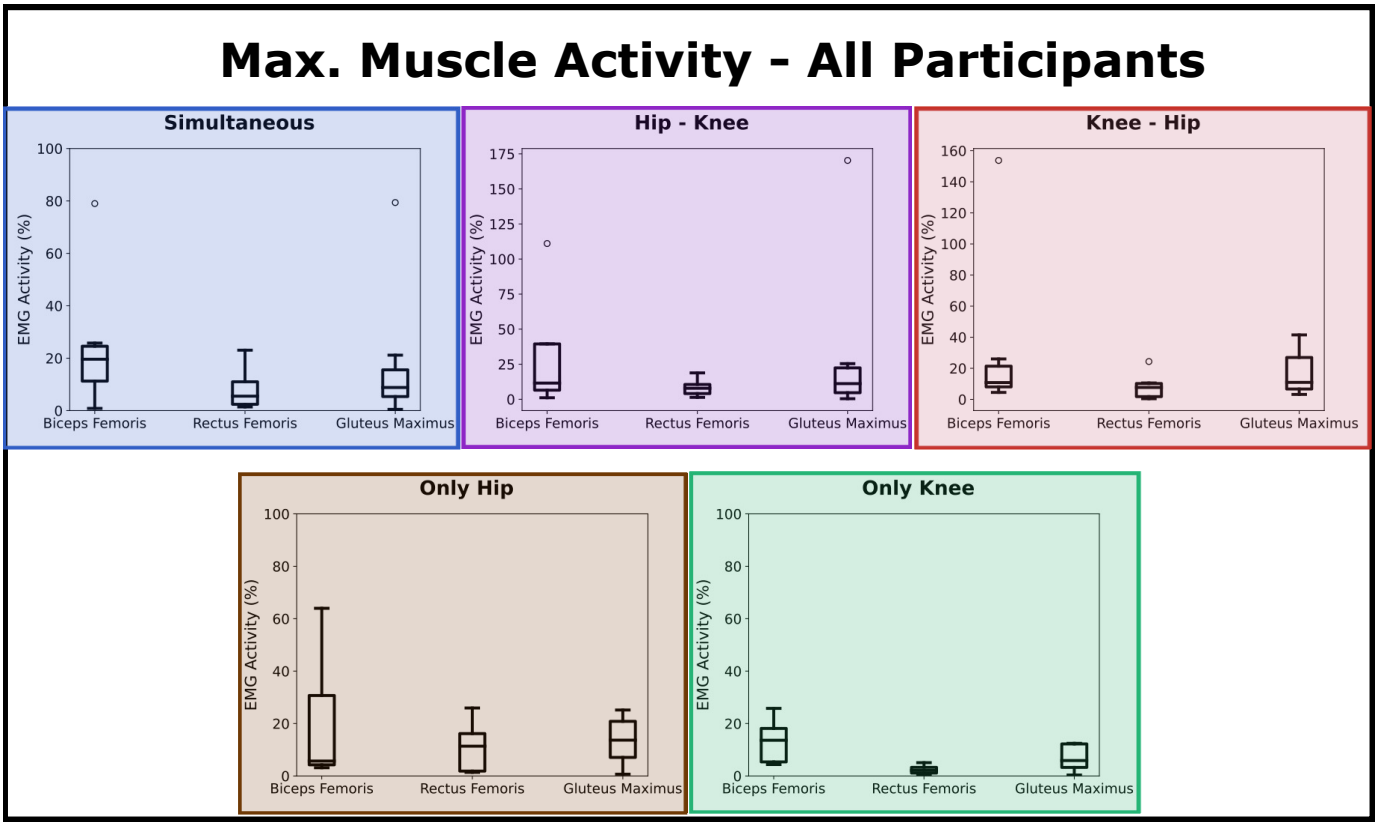

Fig. 11: Maximum muscle activity of the recorded muscles for all participants and controller alternatives. The vertical axes of the plots correspond to the normalized EMG activity, averaged over the three leg elevation repetitions, with respect to the baseline measurement performed at the beginning of the experiment. Most of the participants were able to keep their muscle activity at low levels, while there were also outliers with high muscle activity (e.g. in the ‘hip - knee’ alternative one participant activated his gluteus maximus almost up to 175%). To mimic muscle weakness, the outliers were excluded from the study. Each subplot that corresponds to a specific controller alternative is indicated with the characteristic color that has been used throughout the whole article.

TABLE IV: The table summarizes the participants that were excluded for each controller alternative. The muscle that was activated more than the 25% cut-off threshold is given inside the parenthesis (BF: biceps femoris, RF: rectus femoris, GM: gluteus maximus).

	Excluded Participants
Simultaneous	P2 (BF & RF), P7 (BF & GM)
Hip - Knee	P2 (BF & GM), P6 (BF), P7 (BF & GM)
Knee - Hip	P2 (BF & GM), P7 (BF & GM)
Only Hip	P2 (BF & RF), P6 (BF)
Only Knee	P2 (BF)

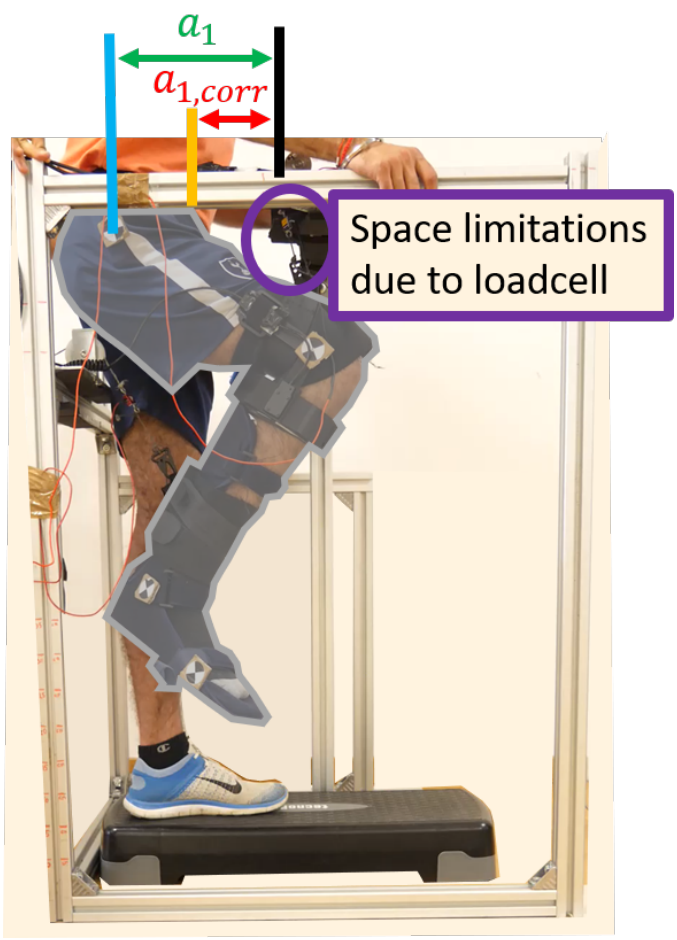

Fig. 12: Picture showing the final position of the leg under the 'small moment arm configuration' of the experimental setup.

2) Tendon forces and velocities: The tendon forces were directly measured by the loadcells. However, as shown in Fig. 12, the body of the participants was getting displaced during the operation of the system, which was non-desirable. The initial position of the hip joint, before the application of forces, was at the orange line of Fig. 12, while the final position was at the blue line. When decomposing the tendon forces, a very small component was responsible for generating hip moment, while the greatest component was responsible for displacing the participant's body. Such a force decomposition happened due to the small angle between the thigh and the tendon at the 'small moment arm configuration'. The displacement of the body resulted in increasing the distance between the motor and the hip joint from $a_{1,corr}$ to a_1 (see Fig. 12). As a result, the data provided by the thigh loadcell would not correspond to the desired moment arms. The same held also for the shank tendon force.

To account for the undesired body displacement effect, we compensated the forces exerted by the tendons numerically. We considered that the tendon-based geometry affects the tendon forces, but not the joint moments. The moments that should be generated at the joints are the same for the same position of the leg. As such, the moments (M_1, M_2) at the displaced position (a_1) are equal to the moments ($M_{1,corr}$, $M_{2,corr}$) at the non-displaced position ($a_{1,corr}$) of the body:

$$M_1 = M_{1,corr} \tag{7}$$

$$M_2 = M_{2,corr} \tag{8}$$

However, the joint moments are linked to the thigh tendon force (F_1) and the shank tendon force (F_2). By combining equations 7, 8 and the expressions of the joint moments with respect to the tendon forces (equations 4, 5), we get the following equations:

$$F_1 \cdot \sin\psi_1 \cdot d_1 - F_2 \cdot \sin\xi \cdot \sqrt{a_2^2 + b_2^2} = F_{1,corr} \cdot \sin\psi_{1,corr} \cdot d_1 - \tag{9}$$

$$-F_{2,corr} \cdot \sin\xi_{corr} \cdot \sqrt{a_{2,corr}^2 + b_{2,corr}^2}$$

$$F_2 \cdot \sin\psi_2 \cdot d_2 = F_{2,corr} \cdot \sin\psi_{2,corr} \cdot d_2 \tag{10}$$

On the left-hand side of the equations, we have the terms that correspond to the displaced position of the body, while on the right-hand side we have the terms that correspond to the non-displaced position of the body (so the 'corr' index refers to the values that would be achieved if the horizontal distance between the hip joint and the motor was $a_{1,corr}$). The variables that are used in the equations are represented in Fig. 6. Here, it should be noted that the distance a_1 of the displaced body position was defined as the distance between the visual marker placed at the hip joint and the hip actuation unit. The value of the distance was manually identified by analyzing the video recordings with the ImageJ software (ImageJ, National Institutes of Health, Bethesda, Maryland, USA). Based on equations 9 and 10, the tendon forces F_1, F_2 are modified to $F_{1,corr}$, $F_{2,corr}$ in order to generate the same amount of moments at the displaced and non-displaced position of the body.

The tendon velocities were calculated by setting in equation 6 the movement time as Δt = 0.3 s, the average time needed for an unimpaired subject to obtain foot clearance during stair climbing [29]. The peak tendon forces and velocities, after the compensation process, are represented in Fig. 13. The

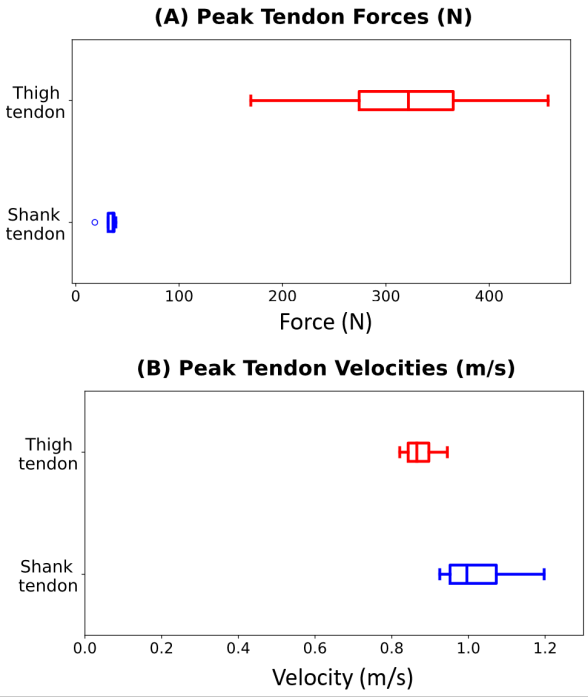

Fig. 13: (A) Peak tendon forces required for leg elevation at the 'small moment arm configuration' of the experimental setup. The thigh tendon needs to apply much higher forces, up to 455 N, than the shank tendon. (B) Peak tendon velocities for leg elevation at the 'small moment arm configuration' of the experimental setup. The shank tendon velocities (0.93 m/s - 1.20 m/s) are a bit higher than the thigh tendon velocities (0.82 m/s - 0.95 m/s).

thigh tendon provided forces up to 455 N and velocities up to 0.95 m/s, while the shank tendon provided forces up to 50 N and velocities up to 1.2 m/s.

3) EMG activity: Residual muscle activity was detected during the experimental procedure with the 'small moment arm configuration' of the experimental setup. We analyzed the data from participants P1, P3, P4, P5 because their normalized muscle activity was lower than the 25% cut-off threshold.

IV. Discussion

In the current study, we built a tendon-driven system to experimentally identify four basic requirements, being the foot clearance, the joint moments, the tendon forces, and the tendon velocities, that the system should provide to lift the foot above a stair-step. When no space constraints were imposed on the experimental setup, the most efficient controller alternative, being the 'simultaneous', provided up to 40.1 Nm at the hip joint and up to 23.2 Nm at the knee joint. After imposing space constraints on the system to mimic a wearable, portable exosuit, the tendon forces and velocities were investigated because they are the critical factors for dimensioning the actuation units of an exosuit. In the portable concept, we found that the highest demands in terms of tendon forces concern the thigh tendon (up to 455 N), while in terms of velocities, the shank tendon (up to 1.2 m/s) required slightly higher velocities than the thigh tendon (up to 0.95 m/s).

A. Big moment arm configuration

1) Foot clearance: Each of the five controller alternatives provided foot clearance greater than the height of most stair-steps [16], when high levels of motor currents were applied. However, the 'hip - knee' and 'only hip' alternatives generated a trajectory in which the foot would collide with the stair-step, if existed during the experiment, see Fig. 8(B). Such a collision would happen because, when first flexing the hip joint, the foot mainly moves anteriorly without having obtained the necessary foot clearance. Similarly, in the 'knee - hip' and 'only knee' alternatives the foot mainly moves posteriorly, resulting in an abnormal leg movement. Able-bodied subjects normally obtain foot-clearance during stair climbing by flexing their hip and knee joints almost simultaneously, hence only the 'simultaneous' alternative was able to better reproduce normal movement.

Walking normally is a consideration that should be taken into account when developing an assistive robot that will be used by patients. From a societal point of view, the person feels more comfortable and well-integrated into the society when looking normal in daily life activities [17]. Moreover, when people walk or climb stairs abnormally, they are more prone to falls, while other health-related problems, such as back pain or arthritis, might also appear [30].

A qualitative comparison between the experimental joint angles, obtained during the 'simultaneous' alternative, and the joint angles of able-bodied subjects during stair climbing reported in [31] is shown in Fig. 14. Differences between the literature data and the kinematic data exist because the experimental conditions are not the same as the ones given in Bannwart et al. [31]. First and foremost, our tendon-driven system provided foot clearance with the subject being fixed in space, while in [31] the subjects were actually climbing a staircase. Furthermore, the achieved foot clearance and the movement time might be different as they are not mentioned in the study that was used for comparison [31]. Another source of errors is the accuracy of the collected experimental data. The experimental angles of the joints were measured with IMU sensors that usually have limited resolution. The comparison would be more reliable if a motion capture system had been used, as has been done in relevant studies [32]. Overall, the kinematic results of the 'simultaneous' alternative are quite promising for next studies that should particularly optimize the timing with which the two actuation units provide support to better resemble normal stair climbing patterns.

2) Moments generated at the joints: The moments provided at the hip were higher than the moments provided at the knee because the hip moments have to compensate for the moments due to the weight of the thigh, the shank, and the foot. On the contrary, the moments at the knee joint have to compensate only for the moments due to the weight of the shank and the foot.

Among the controller alternatives, the highest hip moments are noticed at the 'hip - knee' and 'only hip' alternatives, see

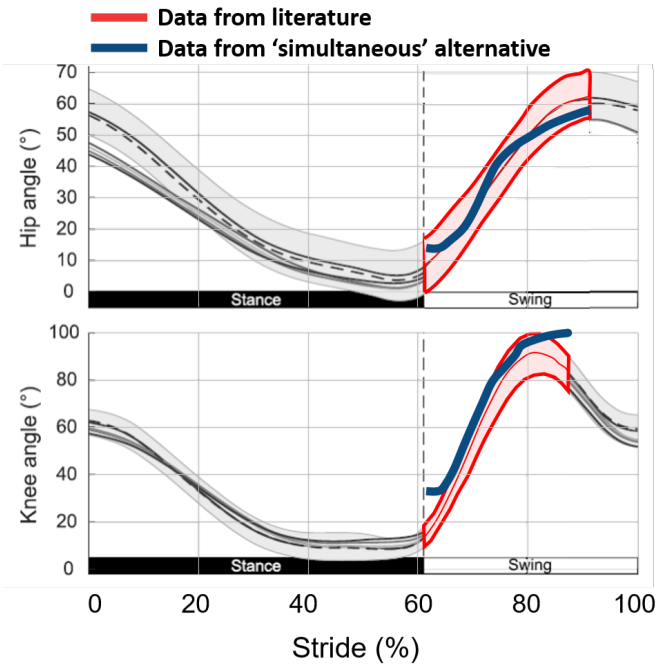

Fig. 14: The plot represents a comparison between the mean of the joint angles obtained from the 'simultaneous' alternative of the experiment and the joint angles achieved by able-bodied subjects during stair climbing. The comparison is done only at the part of the stride where the foot clearance phase takes place. Figure adapted from Bannwart et al. [31].

Fig. 10, because the hip joint is flexed until its final position without any application of forces at the shank. As a result, the shank angle oscillates around 0 deg (the oscillation is due to the dynamics of the leg), while in the 'simultaneous' and 'knee - hip' alternatives the shank is actively pulled by the tendon along with the flexion of the hip joint. As a result, the gravitational forces due to the mass of the shank and the foot in the 'hip - knee' and 'only hip' alternatives create bigger moment arms around the hip joint than in the 'simultaneous' and 'knee - hip' alternatives, consequently higher moments are generated. Regarding the moments provided at the knee joint, they are at similar levels for all alternatives, because they depend on the moment arms of the shank and foot gravitational forces around the knee joint which are similar for all alternatives. Overall, when comparing the five alternatives at each joint individually, higher efficiency at the hip moments is noticed for the 'simultaneous' and 'knee - hip' alternatives, while at the knee moments, the 'simultaneous' and 'hip - knee' alternatives show slightly higher efficiency (both minimum and maximum values of the boxplots were lower). However, when taking into account both joints, the 'simultaneous' alternative has the highest efficiency.

When comparing with other assistive devices reported in the literature, the joint moment results show deviations. The rigid exoskeleton, developed by Farris et al. [33], provided 27.3% higher hip moments and 27.8% lower knee moments than the maximum hip and knee moments that were correspondingly generated by our tendon-driven system when simultaneously flexing both joints. Such deviations are expected because we performed the experiments with unimpaired participants that were instructed to relax their leg, while in [33], the exoskeleton was tested with a paraplegic subject. Moreover, the height of the achieved foot clearance and the movement time were not the same among the two studies. However, we cannot further elaborate on why the hip moment was higher, while the knee moment was lower in Farris et al. [33], as no details about the joints range of motion and the movement time were provided in their study.

When looking into the internal moments, generated by able-bodied subjects during foot clearance, more substantial differences can be noticed. According to Protopapadaki et al. [34], the flexion moments were approximately 10 - 15 Nm at both hip and knee joints. The reported moments correspond to a reduction of approximately 68.8% at the hip and 46.1% at the knee when compared to our experimental findings. Such reductions emerge from the fact that healthy subjects use their ankle during toe-off to achieve foot clearance with a smaller amount of required moments at the hip and knee joints. Consequently, investigating the possibility of assisting ankle plantar flexion at the end of the stance phase to increase the foot clearance would be a valid consideration.

3) EMG activity: When the unimpaired participants were instructed to keep their leg muscles relaxed, they were not able to achieve an absolute absence of muscle activity. However, in most of the cases, their EMG signals were kept at low levels. Muscle relaxation is critical for the current study to mimic the behavior of a person with muscle weakness [35].

However, from the EMG data we cannot conclude whether the residual muscle function works with or against the movement, because the contribution to foot clearance changes from muscle to muscle. More specifically, the activation of the biceps femoris shows that the muscle assisted knee flexion but resisted in hip flexion, because the biceps femoris is knee flexor and hip extensor. Accordingly, the activation of the rectus femoris shows that the muscle assisted hip flexion and resisted in knee flexion, while the activation of the gluteus maximus shows resistance in hip flexion.

Other studies reported in the literature show that people usually have low muscle activity during the foot clearance phase of the stair climbing movement [36]. When looking into the reported EMG data, muscles linked to the hip and knee joints, such as the hamstrings and the rectus femoris are hardly activated. On the contrary, Yali et al. [36], shows that the tibialis anterior, not recorded in our study, had considerable activity. Thus, to have a deeper comprehension of the participants' muscle activities, more muscles should be recorded. It would be important to track mono-articular muscles, such as the iliopsoas, or muscles spanning the ankle joint, such as the tibialis anterior. In that case, a more complex EMG setup would be required with combinations of surface and needle EMG sensors [37].

Overall, with the tendon-driven system in the 'big moment arm configuration', we identified the required joint moments for lifting the foot above a step. The knowledge of the joint moments can be used to combine moment arms with tendon forces, which are critical for the design of an exosuit.

B. Small moment arm configuration

1) Foot clearance: The system at the 'small moment arm configuration' provided 32% lower foot clearance than the 'big moment arm configuration'. The reduced foot clearance limits the applicability of such a system because then it can be used only in places that have shorter stair-steps. Since the reduced foot clearance was due to the space limitation of the thigh tendon, see Fig. 12, the hip actuation unit could be placed at a greater height, approximately above the umbilicus, to increase the winding length of the thigh tendon. However, the disadvantage is that the actuation unit, being in that position, will constrain the movement of the arms. Alternatively, higher knee flexion could be provided to obtain greater foot clearance with the downside of higher deviations from the normal movement.

2) Tendon forces and velocities: The tendon forces and velocities were extracted after performing a correction on the measurements obtained by the sensors. The correction was necessary because, during the application of forces by the tendon-driven system, the body of the participant was displaced, thus changing the moment arms of the tendons around the joints, see Fig. 12. Therefore, we can only have estimations of the tendon forces and velocities that would be required from a wearable, portable exosuit. An improvement that should be done in the experimental setup to account for the undesired body movement is the placement of two horizontal bars that prevent the subject from moving relatively to the motors, as shown in Fig. 15.

Assuming that the performed corrections give us good estimations, the highest requirements for supporting foot clearance with a tendon-driven system concern the thigh tendon. Similarly to the Myosuit [32], forces up to 455 N were exerted at the thigh tendon in order to support hip flexion with a corresponding maximum tendon velocity of 0.95 m/s. On the contrary, the maximum shank tendon forces exerted by the tendon-driven system were 89% lower than the maximum thigh tendon forces, while the velocity at the shank tendon was slightly higher than the velocity at the thigh tendon.

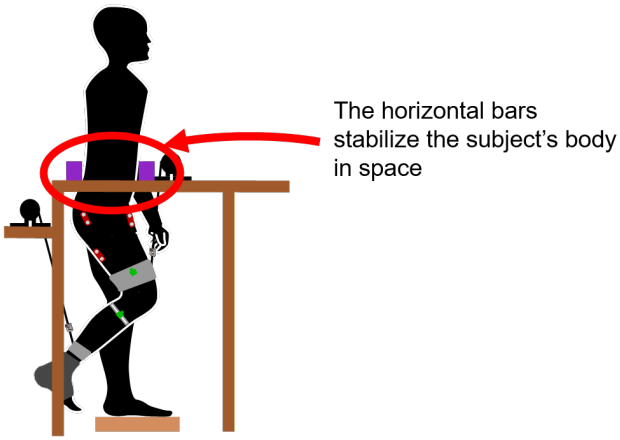

Fig. 15: Recommended improvement of the developed experimental setup. It is suggested that two horizontal bars, demonstrated with purple color, should be added to stabilize the subject's body.

The high required tendon forces and moments of the hip joint in combination with the low required tendon forces and moments of the knee joint can be used to provide insights into potential implementations of exosuits that support foot clearance. The most robust and versatile concept would be to use two actuation units per leg, see Fig. 16(A), because the level and timing of supporting hip flexion and knee flexion can be regulated independently. However, the disadvantage is that the proposed exosuit implements two actuation units per leg, so four in total, resulting in a higher weight of the device.

Alternative implementations of more lightweight systems can be designed by using one motor per leg. According to Bannwart et al. [31], and verified with our experimental data, the hip and knee joints flex at the same time to achieve foot clearance in an efficient and natural way. Consequently, moments have to be provided at the joints simultaneously. Hence, a bi-articular tendon-driven device that uses one artificial tendon to flex both joints, as shown in Fig. 16(B) schematically, would exploit joint synergies [38] to minimize the number of the actuation units. On the downside, the versatility is reduced, because the level and timing of the provided support cannot be independently adjusted for both joints.

Another implementation that has one actuation unit per leg exploits the use of passive elements, such as spring-like components, see Fig. 16(C). The analysis of the tendon forces from our experiment indicated that the hip joint needs to be assisted by high tendon forces, while the knee joint requires

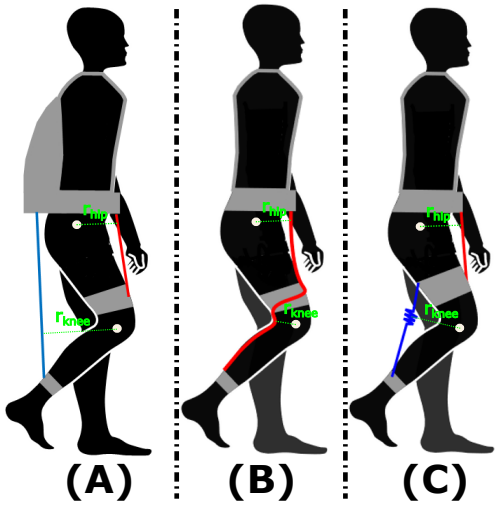

Fig. 16: (A) Potential implementation of a wearable, portable exosuit that uses two actuation units per leg for independent actuation of the hip and knee joints. (B) Proposed bi-articular design of a tendon-driven portable exosuit. The system uses one tendon that creates a hip flexion moment arm (r_{hip}) to pull the thigh and a knee flexion moment arm (r_{knee}) to pull the shank. The exact routing of the tendon should be further investigated. (C) Proposed design of a semi-active tendon-driven exosuit. The system actively supports hip flexion with the thigh tendon (in red), while passively supports knee flexion with a spring-like component (in blue).

low tendon forces. Thus, the actuation unit that supports the knee joint could be potentially replaced by a spring-like component that could passively exert the forces of the shank tendon, as suggested by Haufe et al. [21]. The semi-passive solution reduces the weight of the system, although it has the disadvantage that the passive component would resist in knee extension during other phases of stair climbing.

Nonetheless, the recommended designs are initial suggestions for the implementation of wearable, portable exosuits. Further investigations should be performed for the proper development of such systems. For instance, the determination of the anchor points and the exact routing of the tendon at the bi-articular design have to be carefully examined. Similarly, the exact mechanical properties and the effect of a passive component throughout a whole stride should also be tested experimentally.

3) EMG activity: In the 'simultaneous' alternative of the 'small moment arm configuration' of the experimental setup, four participants in total were excluded from the study due to high levels of muscle activity. That can be explained by the fact that higher forces were applied to lift the foot compared to the 'big moment arm configuration'. As a result. more abrupt movements were performed that impelled the participants to activate their muscles non-voluntarily.

C. Study limitations and future work

The current study showcases a tendon-driven system that provided foot clearance to unimpaired participants, so the results are extracted based on subjects that were instructed to keep their leg relaxed. With this consideration, we identified the moments that the system generated at the joints to support foot clearance. To mimic muscle weakness, we analyzed only data from participants that kept their muscle activity at low levels. However, for greater reliability, it would be favorable to also perform experimental trials with people that have muscle weakness.

Moreover, the experiment was conducted with the person being fixed in space. We expect that the kinematic and kinetic data will differ when the system provides assistance in hip and knee flexion during an actual stair climbing movement because dynamic effects would have a stronger influence. In that case, the climbing speed would play a key role. Therefore, an experiment that investigates assistance during foot clearance with the person navigating stairs at several speeds would provide better insights.

Finally, from a design perspective, the developed experimental setup in the 'small moment arm configuration' was limited due to the relative displacement of the body with respect to the actuation units. Another design iteration should be performed to extract more reliable results.

V. Conclusion

In this study, we presented an experimental approach of how to systematically identify four basic requirements, being the foot clearance, the joint moments, the tendon forces, and the tendon velocities, for developing an exosuit that supports foot clearance during stair climbing. Therefore, we implemented a tendon-driven system that lifts the foot sufficiently for stair navigation, by applying tendon forces at the thigh to flex the hip joint and tendon forces at the shank to flex the knee joint. The system can provide up to 40.1 Nm at the hip and up to 23.2 Nm at the knee when simultaneously flexing both joints, while not being constrained by any space limitations. When modified to mimic a wearable, portable exosuit, the system can provide foot clearance by applying high forces with the thigh tendon and low forces with the shank tendon. Therefore, potential implementations of wearable, portable exosuits should exploit the low required shank tendon forces and the possibility of simultaneously flexing the hip and knee joints. In that way, we can more efficiently assist foot clearance during stair climbing, while minimizing the body protrusion and the number of actuation units.

References

[1] S. Nadeau, B. McFadyen, and F. Malouin, "Frontal and sagittal plane analyses of the stair climbing task in healthy adults aged over 40 years: what are the challenges compared to level walking?" *Clinical Biomechanics*, vol. 18, no. 10, pp. 950–959, 2003.

[2] N. G. Harper, J. M. Wilken, and R. R. Neptune, "Muscle Function and Coordination of Stair Ascent," *Journal of Biomechanical Engineering*, vol. 140, no. 1, Oct. 2017.

[3] A. K. Silverman, R. R. Neptune, E. H. Sinitski, and J. M. Wilken, "Whole-body angular momentum during stair ascent and descent," *Gait Posture*, vol. 39, no. 4, pp. 1109–1114, 2014.

[4] T. Andriacchi, G. Andersson, R. Fermier, D. Stern, and J. Galante, "A study of lower-limb mechanics during stair-climbing," *J Bone Joint Surg Am*, vol. 62, no. 5, pp. 749–57, 1980.

[5] A. Protopapadaki, W. I. Drechsler, M. C. Cramp, F. J. Coutts, and O. M. Scott, "Hip, knee, ankle kinematics and kinetics during stair ascent and descent in healthy young individuals," *Clinical Biomechanics*, vol. 22, no. 2, pp. 203–210, 2007.

[6] J. K. Startzell, D. A. Owens, L. M. Mulfinger, and P. R. Cavanagh, "Stair negotiation in older people: A review," *Journal of the American Geriatrics Society*, vol. 48, no. 5, pp. 567–580, 2000.

[7] A. R. De Asha, "Variability and Distribution of Minimum Toe Clearance in Individuals with Unilateral Transtibial Amputation: The Effects of Walking Speed," *JPO Journal of Prosthetics and Orthotics*, vol. 27, no. 3, pp. 78–83, Jul. 2015.

[8] P. N. Matsuda, A. Shumway-Cook, A. M. Bamer, S. L. Johnson, D. Amtmann, and G. H. Kraft, "Falls in multiple sclerosis," *PMR*, vol. 3, no. 7, pp. 624–632, 2011.

[9] K. Pongpipatpaiboon, M. Mukaino, F. Matsuda, K. Ohtsuka, H. Tanikawa, J. Yamada, K. Tsuchiyama, and E. Saitoh, "The impact of ankle–foot orthoses on toe clearance strategy in hemiparetic gait: a cross-sectional study," *Journal of NeuroEngineering and Rehabilitation*, vol. 15, no. 1, p. 41, Dec. 2018.

[10] R. J. Farris, H. A. Quintero, and M. Goldfarb, "Performance evaluation of a lower limb exoskeleton for stair ascent and descent with Paraplegia," in *2012 Annual International Conference of the IEEE Engineering in Medicine and Biology Society*. San Diego, CA: IEEE, Aug. 2012, pp. 1908–1911.

[11] C. Woods, L. Callagher, and T. Jaffray, "Walk tall: The story of rex bionics," *Journal of Management Organization*, vol. 27, pp. 1–14, Dec. 2018.

[12] M. Xiloyannis, R. Alicea, A.-M. Georgarakis, F. L. Haufe, P. Wolf, L. Masia, and R. Riener, "Soft robotic suits: State of the art, core technologies, and open challenges," *IEEE Transactions on Robotics*, pp. 1–20, 2021.

[13] P. Joudzadeh, A. Hadi, K. Alipour, and B. Tarvirdizadeh, "Design and implementation of a cable driven lower limb exoskeleton for stair climbing," in *2017 5th RSI International Conference on Robotics and Mechatronics (ICRoM)*, 2017, pp. 76–81.

[14] X. Wu, K. Fang, C. Chen, and Y. Zhang, "Development of a lower limb multi-joint assistance soft exosuit," *Science China Information Sciences*, vol. 63, no. 7, pp. 170–207, Jul. 2020.

[15] S. Zhao, Y. Yang, Y. Gao, Z. Zhang, T. Zheng, and Y. Zhu, "Development of a soft knee exosuit with twisted string actuators for stair climbing assistance," in *2019 IEEE International Conference on Robotics and Biomimetics (ROBIO)*, 2019, pp. 2541–2546.

[16] O. of the Deputy Prime Minister, "Protection from falling, collision and impact," http:/www.inbalance-energy.co.uk/building_regulations/, September 1998.

[17] A. Kapeller, M. H. Nagenborg, and K. Nizamis, "Wearable robotic exoskeletons: A socio-philosophical perspective on Duchenne muscular dystrophy research," *Paladyn, Journal of Behavioral Robotics*, vol. 11, no. 1, pp. 404–413, Sep. 2020.

[18] A. T. Asbeck, S. M. D. Rossi, K. G. Holt, and C. J. Walsh, "A biologically inspired soft exosuit for walking assistance," *The International Journal of Robotics Research*, vol. 34, no. 6, pp. 744–762, 2015.

[19] I. Kang, H. Hsu, and A. Young, "The Effect of Hip Assistance Levels on Human Energetic Cost Using Robotic Hip Exoskeletons," *IEEE Robotics and Automation Letters*, vol. 4, no. 2, pp. 430–437, Apr. 2019.

[20] A. T. Asbeck, R. J. Dyer, A. F. Larusson, and C. J. Walsh, "Biologically-inspired soft exosuit," in *2013 IEEE 13th International Conference on Rehabilitation Robotics (ICORR)*. Seattle, WA: IEEE, Jun. 2013, pp. 1–8.

[21] F. L. Haufe, P. Wolf, R. Riener, and M. Grimmer, "Biomechanical effects of passive hip springs during walking," *Journal of Biomechanics*, vol. 98, Jan. 2020.

[22] J. Markowitz and H. Herr, "Human leg model predicts muscle forces, states, and energetics during walking," *PLOS Computational Biology*, vol. 12, no. 5, pp. 1–30, May 2016.

[23] M. Cardona and C. E. García Cena, "Biomechanical analysis of the lower limb: A full-body musculoskeletal model for muscle-driven simulation," *IEEE Access*, vol. 7, pp. 92 709–92 723, 2019.

[24] SENIAM, "Seniam project 2018," http://www.seniam.org/, retrieved June 2021.

[25] M. Halaki and K. Gi, "Normalization of EMG Signals: To Normalize or Not to Normalize and What to Normalize to?" in *Computational Intelligence in Electromyography Analysis - A Perspective on Current Applications and Future Challenges*, G. R. Naik, Ed. InTech, Oct. 2012.

[26] N. Sanchez, A. M. Acosta, R. López-Rosado, A. Stienen, and J. Dewald, "Lower extremity motor impairments in ambulatory chronic hemiparetic stroke: Evidence for lower extremity weakness and abnormal muscle and joint torque coupling patterns," *Neurorehabilitation and Neural Repair*, vol. 31, p. 154596831772197, 08 2017.

[27] C. Kim and J. Eng, "The relationship of lower-extremity muscle torque to locomotor performance in people with stroke," *Physical therapy*, vol. 83, pp. 49–57, 02 2003.

[28] L. Chung, "Muscle weakness in persons with multiple sclerosis," *Open Access Dissertations*, vol. 268, 2010.

[29] J.-H. Choi, E. R. Galea, and W.-H. Hong, "Individual Stair Ascent and Descent Walk Speeds Measured in a Korean High-Rise Building," *Fire Technology*, vol. 50, no. 2, pp. 267–295, Mar. 2014.

[30] W. Pirker and R. Katzenschlager, "Gait disorders in adults and the elderly: A clinical guide," *Wiener klinische Wochenschrift*, vol. 129, no. 3-4, pp. 81–95, Feb. 2017.

[31] M. Bannwart, E. Rohland, C. A. Easthope, G. Rauter, and M. Bolliger, "Robotic body weight support enables safe stair negotiation in compliance with basic locomotor principles," *Journal of NeuroEngineering and Rehabilitation*, vol. 16, no. 1, p. 157, Dec. 2019.

[32] K. Schmidt, J. E. Duarte, M. Grimmer, A. Sancho-Puchades, H. Wei, C. S. Easthope, and R. Riener, "The Myosuit: Bi-articular Anti-gravity Exosuit That Reduces Hip Extensor Activity in Sitting Transfers," *Frontiers in Neurorobotics*, vol. 11, p. 57, Oct. 2017.

[33] R. J. Farris, H. A. Quintero, and M. Goldfarb, "Performance evaluation of a lower limb exoskeleton for stair ascent and descent with Paraplegia," in *2012 Annual International Conference of the IEEE Engineering in Medicine and Biology Society*. San Diego, CA: IEEE, Aug. 2012, pp. 1908–1911.

[34] A. Protopapadaki, W. I. Drechsler, M. C. Cramp, F. J. Coutts, and O. M. Scott, "Hip, knee, ankle kinematics and kinetics during stair ascent and descent in healthy young individuals," *Clinical Biomechanics*, vol. 22, no. 2, pp. 203–210, Feb. 2007.

[35] A. Den Otter, A. Geurts, T. Mulder, and J. Duysens, "Abnormalities in the temporal patterning of lower extremity muscle activity in hemiparetic gait," *Gait Posture*, vol. 25, no. 3, pp. 342–352, 2007.

[36] H. Yali, S. Ai-guo, G. Haitao, and Z. Songqing, "The muscle activation patterns of lower limb during stair climbing at different backpack load." *Acta of bioengineering and biomechanics*, vol. 17 4, pp. 13–20, 2015.

[37] E. Katsavrias, E. Primetis, and N. Karandreas, "Iliopsoas: A new electromyographic technique and normal motor unit action potential values," *Clinical Neurophysiology*, vol. 116, no. 11, pp. 2528–2532, 2005.

[38] B. J. Stetter, M. Herzog, F. Möhler, S. Sell, and T. Stein, "Modularity in motor control: Similarities in kinematic synergies across varying locomotion tasks," *Frontiers in Sports and Active Living*, vol. 2, p. 168, 2020.

[39] D. A. Winter, *Biomechanics and motor control of human movement*, 4th ed. Hoboken, N.J: Wiley, 2009.

APPENDIX

A. Development process of the experimental setup

In this appendix, we provide the detailed process that was followed to develop the experimental setup. According to a simplified version of the V-model approach of the System Development Life Cycle, we first identified the needs that the setup should cover. The needs were extracted from the project's goals, which were to provide foot clearance in five alternative ways, quantify the kinematic and kinetic behavior of the leg, ensure that muscle weakness is mimicked by able-bodied subjects, and ensure that safety is preserved during the whole experimental procedure. From each need, one or more design requirements were identified, while from each design requirement, one or more system specifications were extracted. Table V summarizes the needs, the design requirements, and the specifications of the system.

TABLE V: Needs, design requirements, and system specifications for the experimental setup. From each need, one or more design requirements are derived, while from each design requirement, one or more system specifications are derived, according to the V-model approach. A color code is used to group the design requirements and the system specifications that correspond to a specific need.

Needs	Design Requirements	System Specifications
(i) We need to perform an experiment in which foot clearance is achieved in different ways with a tendon-driven system	(A) The system shall ensure sufficient foot clearance for stairs navigation of a swinging leg	(1) Thigh angle up to 80 deg
		(2) Shank angle up to 100 deg
		(3) Left foot raised by 10cm from ground level, so that right foot is not in contact with the ground
	(B) The system shall be tendon-driven	(4) Artificial tendons that withstand at least 700 N of tensile forces
		(5) Integration of interface between the human leg and the artificial tendons
	(C) The system shall actively support hip and knee flexion and passively support ankle dorsiflexion	(6) External application of tendon forces up to 350 N at the thigh to support hip flexion
		(7) External application of tendon forces up to 175 N at the shank to support knee flexion
		(8) Ankle joint fixed at 0 deg
		(9) Micro-computer that controls the tendon forces
		(10) Micro-computer that sends and receives signals with a frequency of 100 Hz
	(D) The system shall be available for users with weights ranging from 50-95kg and heights ranging from 150-195cm	(11) Mechanism that places the motors up to a height of 120cm from ground
		(12) Adjustable interface between human leg and artificial tendons - material with low Young modulus (app. 10 MPa) and high elongation (app. 500%)
(ii) We need to understand how the leg moves while obtaining foot clearance and what joint moments are required	(E) The system shall measure the angles of the thigh and the shank	(13) 2 IMU sensors that record the thigh angle and the shank angle respectively
	(F) The system shall measure the tendon forces	(14) Load cell that records tensile forces
		(15) Minimum capacity of loadcell 350 N
		(16) Maximum resolution of loadcell 1 N
(iii) The experiment will be performed with unimpaired participants; however, we need to extrapolate our results to persons with muscle weakness at their lower limbs	(G) The system shall record the activity of muscles involved in hip and knee flexion	(17) EMG sensors to record muscle activity
		(18) Maximum resolution of EMG sensors 2μV
		(19) Minimum sampling frequency of EMG sensors 100Hz
(iv) Safety of the participants should be ensured during the whole experimental procedure	**(H) The system shall mitigate mechanical risks, electrical risks, structural risks, fall risks**	**(20) For mechanical risks mitigation, cushioning in locations of possible collision of the foot with the system**
		(21) For electrical risks mitigation, battery enclosed in a box and cables shielded with insulation tape
		(22) For structural risks mitigation, mechanical structure that consists of components with high load bearing capacity, up to 1000N
		(23) For fall risks mitigation, structure that implements handrails, so that the users can support themselves
	(I) The system shall implement software and hardware stops	(24) Deactivation of system when thigh angle exceeds 100 deg or shank angle exceeds 120 deg
		(25) Deactivation of system when applied forces exceed 350N
		(26) Deactivation of system after user's request
		(27) Hardware stops to prevent the system to further pull on the thigh or the shank

The specific design choices for the development of the experimental setup were extracted from the system specifications. The important specifications will be analyzed:

- Specifications 1 and 2 concerned the angles of the leg segments that were necessary for lifting the foot above a stair-step (more than 22 cm). The values of the angles were calculated from the equations 2 and 3 by taking into account anthropometric data from Winter [39].
- Specification 3 was necessary to create the conditions of a swinging leg. A very simple solution was applied for this specification with the use of a stepper 10 cm tall.
- Specifications 4, 6, and 7 concerned the realization of the tendon-driven setup that should be able to sufficiently lift the foot. The forces were initially estimated from the simple model given in Appendix B, however, a big safety factor (approximately 5) was taken into account to ensure that the leg could be lifted. The solution to these specifications was the incorporation of a 70 W actuation unit (Maxon DC motor EC-i40 + gearbox with 15.16:1 ratio + pulley with 38mm effective diameter) and the use of Dyneema cables (Dyneema Throwline / Marlow, 0.6mm, min. break load 410kg), available infrastructure from MyoSwiss AG.
- Specification 8 required the stabilization of the ankle joint at its neutral position. This specification was implemented with an off-the-shelf ankle-foot orthosis.
- Specifications 9 and 10 were necessary for the active support of hip and knee flexion. The solution was one ARM A8 micro-computer unit (Bea-gleBone; AM335x 1GHz ARM Cortex-A8; programming language C).
- Specification 11 was necessary for experimenting with participants of heights from 150-195 cm. Based on the anthropometric data from Winter [39] for such a height range, we determined the maximum height at which the actuation units should be placed. By integrating a small safety factor, a mechanical frame with a maximum height of 120 cm was built, see Fig. 17. With the use of bolt-nut

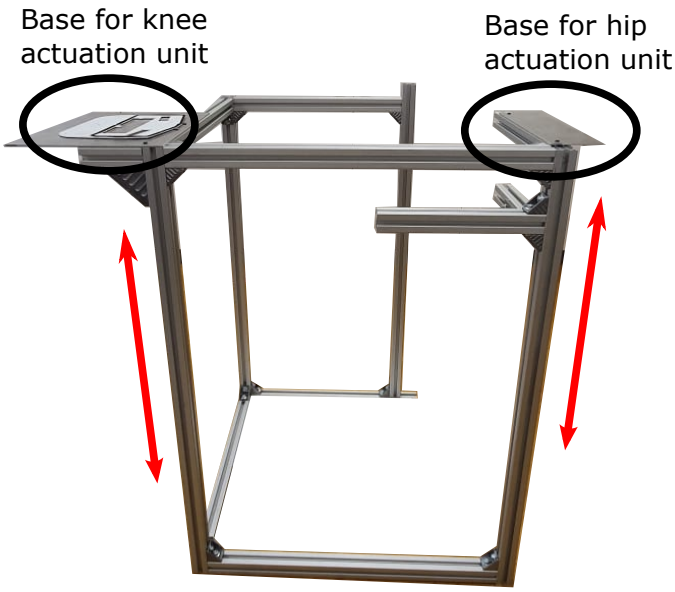

Fig. 17: Mechanical frame of the experimental setup. The height of the actuation units can be adjusted, as indicated by the red arrows. The maximum height at which the actuation units can be placed is 120 cm.

pairs, we were able to modify the height of the actuation units.

- Specifications 5 and 12 were necessary for creating the interface between the experimental setup and the human leg. The interface was implemented with two wearable braces at the thigh and the shank respectively. The material of the braces is synthetic rubber to comply with many leg thicknesses. The braces were fabricated by readjusting an off-the-shelf knee brace, see Fig. 18.
- Specifications 13-19 were necessary for collecting sensor data that later were post-processed. There was no need to create a feedback loop during the experiment with the sensor data, therefore no extremely big resolution was required. Those specifications were fulfilled with the use of 2 simple IMU sensors, 2 S-type loadcells (FUTEK, LSB200/QSH01905, Miniature S-beam Jr.), and 3 EMG sensors (Ultium EMG Sensor System, Noraxon, Scottsdale, AZ, USA).
- Specifications 24-27 were necessary for ensuring safety during the experiment. Specifications 24 and 25 were implemented by coding software thresholds that deactivated the actuation units in case of emergency. The thresholds were responsible for preventing the leg from reaching non-comfortable positions. Specification 26 was implemented with the use of an emergency button, see Fig. 19, while for the hardware stops of specification 27, two knobs were implemented at the tendons.

Based on those considerations, the experimental setup was built, as described in Section II-A.

B. Static tendon-driven model

The static tendon-driven model was developed for three reasons:

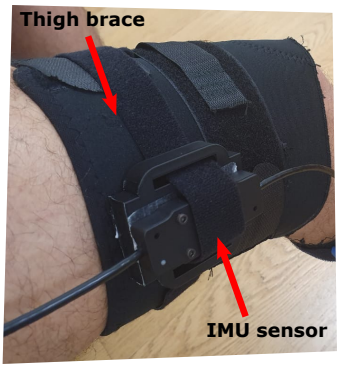

Fig. 18: Thigh brace that implemented the interface between the experimental setup and the human leg. An IMU sensor was attached to record the thigh angle at the sagittal plane.

Fig. 19: Remote controller that implemented an emergency button (shown in red) for deactivating the system when needed.

- To obtain an initial estimation of the motor currents that should be applied by the actuation units for foot clearance. Since the model was static, the predicted currents underestimated the real ones. The underestimation of the motor currents was compensated by scaling them up during the experiment. Yet, the model was useful to inform us about the ratio with which the hip motor current and the knee motor current should be provided.
- To determine the positions of the actuation units. Due to the simplified nature of the model, we could not precisely predict the magnitude of the forces that the actuation units should provide. However, we could specify the positions that we should place the actuation units to efficiently transfer the forces exerted by the tendons to moments at the joints.
- To process the experimental data. The data processing included calculating the trajectory of the foot from IMU data, calculating the moments generated at the joints from the loadcell data, and calculating the tendon velocities from the Hall sensor data. The calculations could be given

by the model because they were based on the tendon-driven geometry. As a result, they were not affected by the static nature of the model.

Since the tendon forces were determined experimentally, a static model that neglected the tissue stiffness of the leg segments, the resistance at the joints, and the dynamic phenomena during the leg's movement would suffice. Nonetheless, the equations that link the joint angles with the displacement of the foot, the tendon forces with the moments at the joints, and the tendon velocities with the motor counts should be precise for reliable data processing.

The model, represented in Fig. 20, was developed according to anthropometric data provided by Winter [39] for a human with a weight of 80kg and a height of 180cm. Table VI summarizes the parameters of the model. Each leg segment, i.e. the thigh, the shank, and the foot, was modelled as a rigid link, the hip and knee joints were assumed to be frictionless, while the ankle joint was fixed at 0 deg. The kinematic behavior, the static behavior, and the tendon-based geometry of the model were analyzed to derive all the necessary equations.

1) Kinematics: To adequately describe the kinematic behavior of the swinging leg during the foot clearance phase, the displacement of the foot along with the corresponding thigh and shank angles should be determined. According to standards

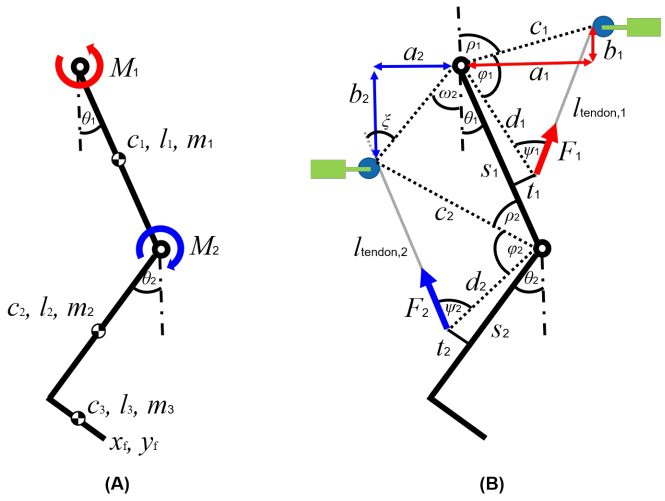

Fig. 20: (A) Representation of a swinging leg in the sagittal plane, along with the parameters (mass, length, CoM) of each leg segment. The thigh, the shank, and the foot were modeled as rigid links. The hip and knee joints were considered frictionless. The ankle joint was fixed at 0 deg. (B) Representation of the model engaged with the tendons, grey lines, and the actuation units. Each actuation unit consisted of a motor, a gearbox (both are shown in green), and a pulley (shown as a blue circle). It should be noted that t_1 and t_2 were used to account for the thickness of the thigh and the shank. Overall, we intended to determine the moments and the forces experimentally, therefore a model that neglected the tissue stiffness of the leg segments, the resistance at the joints, and the dynamic phenomena during the leg's movement would suffice.

TABLE VI: Parameters of the mechanical model. For each of the leg segments, the CoM, the length, and the mass are given, according to Winter [39]. The value of the location of CoM corresponds to the fraction of the CoM distance from the proximal joint to the segment length.

	Location of CoM	Length	Mass
Thigh	$c_1 = 0.433$	$l_1 = 44cm$	$m_1 = 8.0kg$
Shank	$c_2 = 0.606$	$l_2 = 51cm$	$m_2 = 3.7kg$
Foot	$c_3 = 0.500$	$l_3 = 24cm$	$m_3 = 1.2kg$

from several countries [16], the typical height of a stair-step can reach up to 22cm. Integrating a small safety factor, our target value of the required foot clearance was set to 25cm. To determine the thigh (θ_1) and shank (θ_2) angles, two simple kinematic equations, that express the position of the foot (x_f, y_f) with respect to the angles (θ_1, θ_2), were used:

$$x_f = l_1 \cdot \cos\theta_1 + l_2 \cdot \cos\theta_2 + l_3 \cdot \sin\theta_2 \tag{11}$$

$$y_f = l_1 \cdot \sin\theta_1 - l_2 \cdot \sin\theta_2 + l_3 \cdot \cos\theta_2 \tag{12}$$

By implementing a vertical trajectory of the foot tip, the equations 11 and 12 were solved, by applying inverse kinematics, to calculate the angles θ_1 and θ_2. The displacement of the foot and the angles of the leg segments are shown in Fig. 21. Finally, the foot clearance (FC) was determined by calculating the height difference of the foot tip at the final position of the leg and the zero ground level, which was considered to be the stepper:

$$FC = l_1 + l_2 - x_f \tag{13}$$

2) Statics: The goal of the static analysis was to provide a first estimation of the moments required at the joints for elevating the leg. According to the model, the joint moments should compensate for the gravitational forces due to the mass of the leg segments, because the resistance at the joints, the tissue stiffness of the leg segments, and the dynamic phenomena were neglected. The static equations are given by:

$$M_1 = m_1 \cdot g \cdot c_1 \cdot l_1 \cdot \sin\theta_1 + m_2 \cdot g \cdot (l_1 \cdot \sin\theta_1 - c_2 \cdot l_2 \cdot \sin\theta_2) \tag{14}$$
$$+ m_3 \cdot g \cdot (l_1 \cdot \sin\theta_1 - l_2 \cdot \sin\theta_2 + c_3 \cdot l_3 \cdot \cos\theta_2)$$

$$M_2 = m_2 \cdot g \cdot c_2 \cdot l_2 \cdot \sin\theta_2 + m_3 \cdot g \cdot (l_2 \cdot \sin\theta_2 - c_3 \cdot l_3 \cdot \cos\theta_2) \tag{15}$$

3) Tendon-based geometry: The equations that link the joint moments, required due to the gravitational forces of the leg segments, with the tendon forces provided by the actuation units were based on the geometrical configuration of the model, represented in Fig. 20(B). In particular, the hip moment

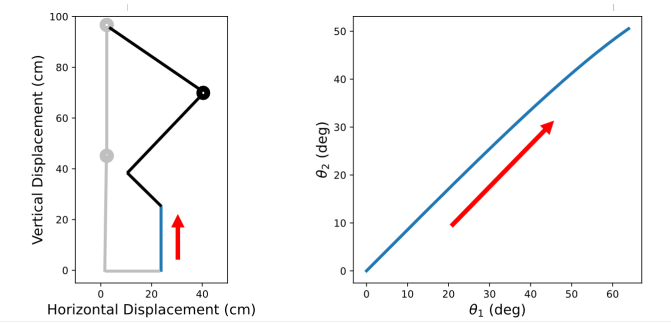

Fig. 21: (A) Displacement of the foot at the 2D space. The blue line, set to be vertical, shows the displacement of the foot during the foot clearance phase. The leg is indicated with grey color at the initial configuration and black color at the final configuration. The red arrow shows the direction of the movement. (B) Thigh and shank angles of the leg that correspond to the vertical movement of the foot. The blue line shows the progression of the angles θ_1 and θ_2. The red arrow shows the direction of the movement.

M_1 is the result of a flexion moment, due to the thigh tendon, and an extension moment, due to the shank tendon. Accordingly, the knee moment M_2 is the result of a flexion moment due to the shank tendon. The mathematical expressions are given by the following equations:

$$M_1 = F_1 \cdot \sin\psi_1 \cdot d_1 - F_2 \cdot \sin\xi \cdot \sqrt{a_2^2 + b_2^2} \tag{16}$$

$$M_2 = F_2 \cdot \sin\psi_2 \cdot d_2 \tag{17}$$

where

$$\cos\psi_1 = \frac{d_1^2 + l_{tendon,1}^2 - c_1^2}{2 \cdot d_1 \cdot l_{tendon,1}} \tag{18}$$

$$l_{tendon,1} = \sqrt{c_1^2 + d_1^2 - 2 \cdot c_1 \cdot d_1 \cdot \cos\phi_1} \tag{19}$$

$$\phi_1 = 180^o - \left(\theta_1 + \tan^{-1}\frac{t_1}{s_1} + \rho_1\right) \tag{20}$$

$$\tan\rho_1 = \frac{a_1}{b_1} \tag{21}$$

$$d_1 = \sqrt{s_1^2 + t_1^2} \tag{22}$$

$$c_1 = \sqrt{a_1^2 + b_1^2} \tag{23}$$

$$\xi = \omega_2 + \psi_2 - \theta_2 - \tan^{-1}\frac{t_2}{s_2} \tag{24}$$

$$\cos\psi_2 = \frac{d_2^2 + l_{tendon,2}^2 - c_2^2}{2 \cdot d_2 \cdot l_{tendon,2}} \tag{25}$$

$$l_{tendon,2} = \sqrt{c_2^2 + d_2^2 - 2 \cdot c_2 \cdot d_2 \cdot \cos\phi_2} \tag{26}$$

$$\phi_2 = 180^o - \left(\theta_1 + \theta_2 + \tan^{-1}\frac{t_2}{s_2} + \rho_2\right) \tag{27}$$

$$\rho_2 = \tan^{-1}\frac{l_1 \cdot \sin\theta_1 + a_2}{l_1 \cdot \cos\theta_1 - b_2} - \theta_1 \tag{28}$$

$$d_2 = \sqrt{s_2^2 + t_2^2} \tag{29}$$

$$c_2 = \sqrt{a_2^2 + b_2^2 + l_1^2 - 2 \cdot l_1 \cdot \sqrt{a_2^2 + b_2^2} \cdot \cos(\theta_1 + \omega_2)} \tag{30}$$

$$\tan\omega_2 = \frac{a_2}{b_2} \tag{31}$$

Here, it should be noted that the variables M_1 and M_2 are the same for the equations 14-17. However, equations 14 and 15 take into account the gravity contributions, while equations 16 and 17 take into account the cable contributions. When all four equations are combined we obtain the static equilibrium (zero total moment).

To determine the tendon forces that were required to generate the moments derived from the static model, we solved the equations 4 and 5 for F_1 and F_2. The tendon forces depend on the positions of the actuation units with respect to the hip joint (a_1, b_1, a_2, b_2), the attachment lengths s_1, s_2, and the thicknesses of the leg segments t_1, t_2. To simplify the analysis, we fixed the vertical positions of the actuation units with respect to the hip joint as $b_1 = 5cm$ and $b_2 = 9cm$. Moreover, we assumed that the thickness of the thigh and the shank were constant ($t_1 = 7cm$ and $t_2 = 5.5cm$). Then we investigated for which values of the variables s_2 and a_2 could we obtain the moment M_2 with lower shank tendon forces. As shown in Fig. 22(A), the force gets smaller as s_2 increases and a_2 decreases. Based on that, we selected $a_2 = 17cm$, $s_2 = 36cm$ taking also into account physical constraints of the leg. Finally, for the selected variables, we investigated for which values of the variables s_1 and a_1 could we obtain the moment M_1 with lower thigh tendon forces. As shown in Fig. 22(B), the force gets smaller as a_1 and s_1 increase. Based on that, we selected $a_1 = 38cm$, $s_1 = 38cm$ taking also into account physical constraints of the leg. For instance, we could have selected even bigger values of a_1 and s_1 to obtain lower tendon forces, however in that case the attachment point would be very close to the knee joint, which was not desirable.

The forces F_i of the tendons can be applied by the actuation units when controlling the motor currents I_i. According to the specifications of the actuation unit, the motor current was calculated by:

$$I_i = \frac{F_i \cdot r_{pulley}}{\eta \cdot \mu \cdot k_M \cdot i_{gb}} \tag{32}$$

where $r_{pulley} = 19mm$ is the effective radius of the pulley, $\eta = 0.89$ is the motor efficiency, $\mu = 0.81$ is the gearbox efficiency, $k_M = 46.1mNm/A$ is the motor torque constant, and $i_{gb} = 15.16$ is the gearbox ratio.

Accordingly, the average velocity v_i of the tendon was calculated from the motor counts c_i given by the Hall sensor as:

$$v_i = \frac{c_i \cdot r_{pulley}}{2\pi \cdot i_{gb} \cdot \Delta t} \tag{33}$$

where Δt is the total movement time.

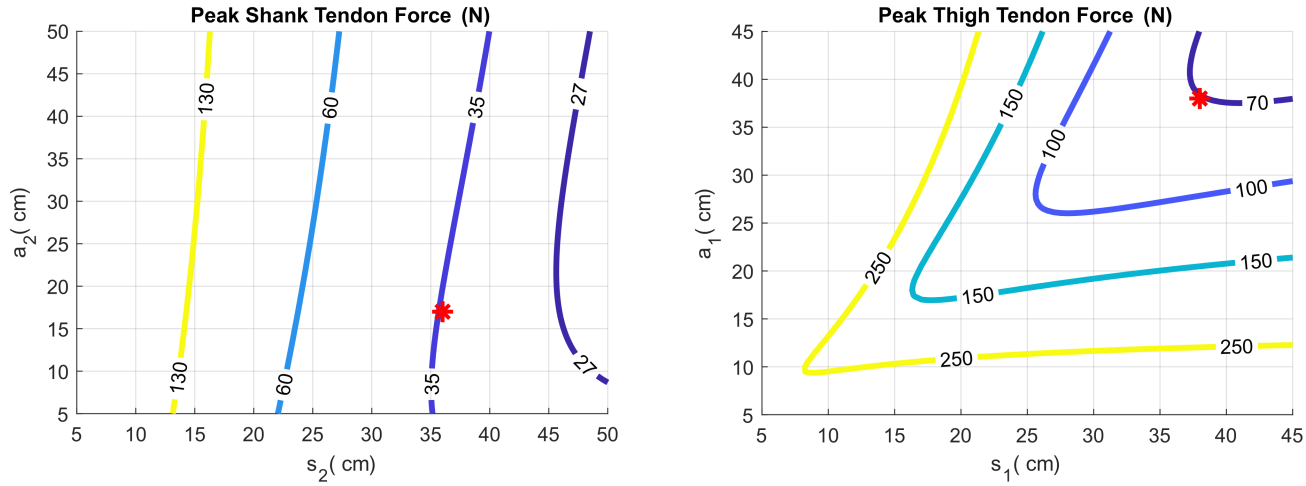

Fig. 22: Contour plot with the peak forces at thigh and shank tendons according to the model. With the term peak, we mean the maximum force exerted at the tendon during the whole movement of the leg. (A) The peak forces of the shank tendon are given for several values of s_2 and a_2. The force gets smaller as s_2 increases and a_2 decreases. Therefore, high s_2 and low a_2 were selected (shown with the red asterisk), taking also into account physical constraints of the leg. (B) The peak forces of the thigh tendon are given for several values of s_1 and a_1 (with s_2 and a_2 selected according to (A)). The force gets smaller as the values of the variables increase. Therefore, the values were selected to be high (shown with the red asterisk), taking also into account the physical constraints of the leg.

C. Data of study participants

TABLE VII: Data of study participants. The following parameters are defined as: l_1 = length from greater trochanter to lateral epicondyle; l_2 = length from lateral epicondyle to calcaneus; l_3 = length from talus to distal phalanx (great toe); C_1 = circumference of thigh at the attachment point of the thigh brace; C_2 = circumference of shank at the attachment point of the shank brace; s_1 = distance of thigh brace's attachment point from greater trochanter; s_2 = distance of shank brace's attachment point from lateral epicondyle.

	Gender	**Age (yrs)**	**Weight (kg)**	**Height (cm)**	l_1 **(cm)**	l_2 **(cm)**	l_3 **(cm)**	C_1 **(cm)**	C_2 **(cm)**	s_1 **(cm)**	s_2 **(cm)**
P1	Female	25	53.7	161	42	46	19	48	39	33	30
P2	Female	24	55.4	163	41	44	19	47	37	30	27
P3	Female	28	65.2	173	42	50	19	46	42	35	30
P4	Male	30	85.7	195	44	56	24	50	38	37	36
P5	Male	24	50.9	163	35	49	21	40	38	30	30
P6	Male	25	68.3	173	40	52	19	47	39	31	30
P7	Male	30	71.7	179	43	53	22	49	38	34	33
P8	Female	29	67.0	176	41	50	21	47	37	35	33